MISCELLANEOUS PAPER N-68-4

PRESSURE DISTRIBUTION ON A BURIED FLAT PLATE SUBJECTED TO STATIC AND AIRBLAST OVERPRESSURES

by

J. P. Balsara

R. S. Cummins, Jr.

October 1968

Sponsored by

Defense Atomic Support Agency

Conducted by

U. S. Army Engineer Waterways Experiment Station

CORPS OF ENGINEERS

Vicksburg, Mississippi

MISCELLANEOUS PAPER N-68-4

PRESSURE DISTRIBUTION ON A BURIED FLAT PLATE SUBJECTED TO STATIC AND AIRBLAST OVERPRESSURES

by

J. P. Balsara

R. S. Cummins, Jr.

October 1968

Sponsored by

Defense Atomic Support Agency

Conducted by

U. S. Army Engineer Waterways Experiment Station

CORPS OF ENGINEERS

Vicksburg, Mississippi

ARMY-MRC VICKSBURG, MISS.

FOREWORD

This paper was prepared for presentation at the American Society of Civil Engineers Structural Engineering Conference to be held in Pittsburgh, Pennsylvania, in September 1968.

The research reported herein was sponsored by the Defense Atomic Support Agency and conducted under the general direction of Mr. G. L. Arbuthnot, Jr., Chief of the Nuclear Weapons Effects Division, and under the direct supervision of Mr. W. J. Flathau, Chief of the Protective Structures Branch. COL Levi A. Brown, CE, is the Director and Mr. J. B. Tiffany is the Technical Director of the Waterways Experiment Station.

The writers wish to express their appreciation to Messrs. P. K. Ho and P. J. Rieck for their efforts in formulating the computer programs used in this study.

SUMMARY

The objectives of this study were to develop and represent the pressure distribution on the surface of a buried, simply supported flat plate subjected to static and airblast overpressures. The plate was 24 in. square and buried in dense, dry sand to a depth of one-half span, and subjected to static surface overpressures ranging from 0 to 75 psi and airblast overpressures at the surface ranging from 29 to 65 psi. The plate was instrumented with thirteen soil-stress gages to measure the soil-stress or pressure distribution, and a load cell was used to measure the total reaction of the plate. A surface represented by a third order polynomial was fitted to the experimental data to represent graphically the pressure distribution and to facilitate the computation of the value (force) of the volume under the surface so that it could be compared with the value of force measured by the reaction load cell. The results indicate that the load on the plate, for both the static test and the dynamic test for times when the comparison was valid, was considerably greater than the reaction. The static soil stress, represented in nondimensional form as the ratio of soil stress to overpressure, remains relatively constant during loading but increases during unloading. The dynamic soil-stress overpressure ratio, above a certain overpressure level, increases from below unity at the center of the plate to above unity at the supports, and the distribution and variation with time essentially remain the same.

PRESSURE DISTRIBUTION ON A BURIED FLAT PLATE SUBJECTED TO STATIC AND AIRBLAST OVERPRESSURES

J. P. Balsara[1]

R. S. Cummins, Jr.[2]

INTRODUCTION

The redistribution of pressure on a buried structure subjected to the blast effects of nuclear weapons is dependent on the surface pressure-time history, the geometry and flexibility of the structure, and the soil characteristics. The basic problem from an analytical or numerical approximation standpoint is to formulate a mathematical model that describes the pressure transmitted to the structure. Experimentally the problem is that of measuring stresses at discrete locations on the surface of the structure with transducers that do not influence the magnitude of the pressure recorded at such locations. For an ideal case, a precise measurement requires that a gage deform in exactly the same manner as the structure at each gage location. The gage itself behaves as a small structure and the load distribution over its surface is affected by the deformation characteristics of the gage relative to the structure. The development and evaluation of some of the on-structure stress gages used in protective structures research are

---

[1]Project Manager, Projects Group, Protective Structures Branch, Nuclear Weapons Effects Division, U. S. Army Engineer Waterways Experiment Station.

[2]Structural Engineer, Projects Group, Protective Structures Branch, Nuclear Weapons Effects Division, U. S. Army Engineer Waterways Experiment Station.

reported by Faust and Ingram (4), and Reiff and Linger (11).

In a buried configuration, a structure with a cylindrical geometry redistributes the pressure to transmit it primarily by a compressive mode thereby increasing its load-carrying capacity, as discussed by Meyer and Flathau (9) and Dorris (2). For flat slab-type structures, redistribution of pressures results in redistributions of shearing forces and bending moments, not necessarily beneficial to structural response.

This study was primarily intended as the first phase in an experimental modeling program concerning buried, simply supported, reinforced concrete slabs subjected to airblast overpressures. Since scaled response is dependent on proper scaling of pressure-time loading inputs, it was considered necessary to investigate first the redistribution of stress on the outer surface of the buried structure caused by both static and transient airblast loadings applied to the soil surface.

The objective of this study was to develop a procedure to measure and represent graphically the pressure distribution on the surface of a buried, simply supported, flat plate, showing variation of pressure with time.

For this study only tests in dense, dry sand were conducted with the depth of burial of the plate equal to one-half the span for both static and airblast overpressure loadings that caused the plate to respond elastically. However, in-place calibration tests were conducted at zero depths of burial. The results from one dynamic test at zero depth of burial, and one static run and three dynamic tests at one-half span depth of burial are presented.

EXPERIMENTAL PROCEDURE

The on-structure soil-stress gage used in this investigation was developed at the Waterways Experiment Station (WES). The gage, shown in Fig. 1, is of the column type constructed from 6061-T6 aluminum alloy with a rectangular column section of 0.375 in. by 0.045 in. and a column length of 1 in. The diameter of the circular loading head is 0.5 in. A full strain-gage bridge was used by placing two gages along the load axis and two gages in the transverse direction.

At an incident pressure of 100 psi, the true strain, ϵ_y , in the column is 116 μin./in. The apparent strain output from a bridge hooked up as described above is

$$\epsilon_a = 2\epsilon_y(1 + \nu)$$

If Poisson's ratio, ν , is taken as 0.33, then ϵ_a = 312 μin./in.

The entire test assembly, shown in Fig. 2, consisted of a 0.67-in.-thick steel plate instrumented with 13 soil-stress gages and simply supported on a load collector fabricated from fiber-glass-reinforced resin. The assembly was supported on a single load cell and inclosed in a rectangular steel box. The load cell, which has a diameter of 1.625 in., can produce an apparent strain output of 2463 μin./in. for a 100-psi applied loading. To meet the simply supported boundary conditions, the four corners of the plate were held down by a bolt-pin assembly which prevented the corners from rising but at the same time allowed horizontal movement.

The tests were conducted in the Blast Load Generator (BLG) facility at WES described by Flathau (5). The Small Blast Load Generator (SBLG), shown in Fig. 3, is a 4-ft-diam facility which consists of stacked rings capped with a static or dynamic bonnet. The rings can be stacked over a 9.5-ft soil column below floor level or on a rigid base at floor level. A more

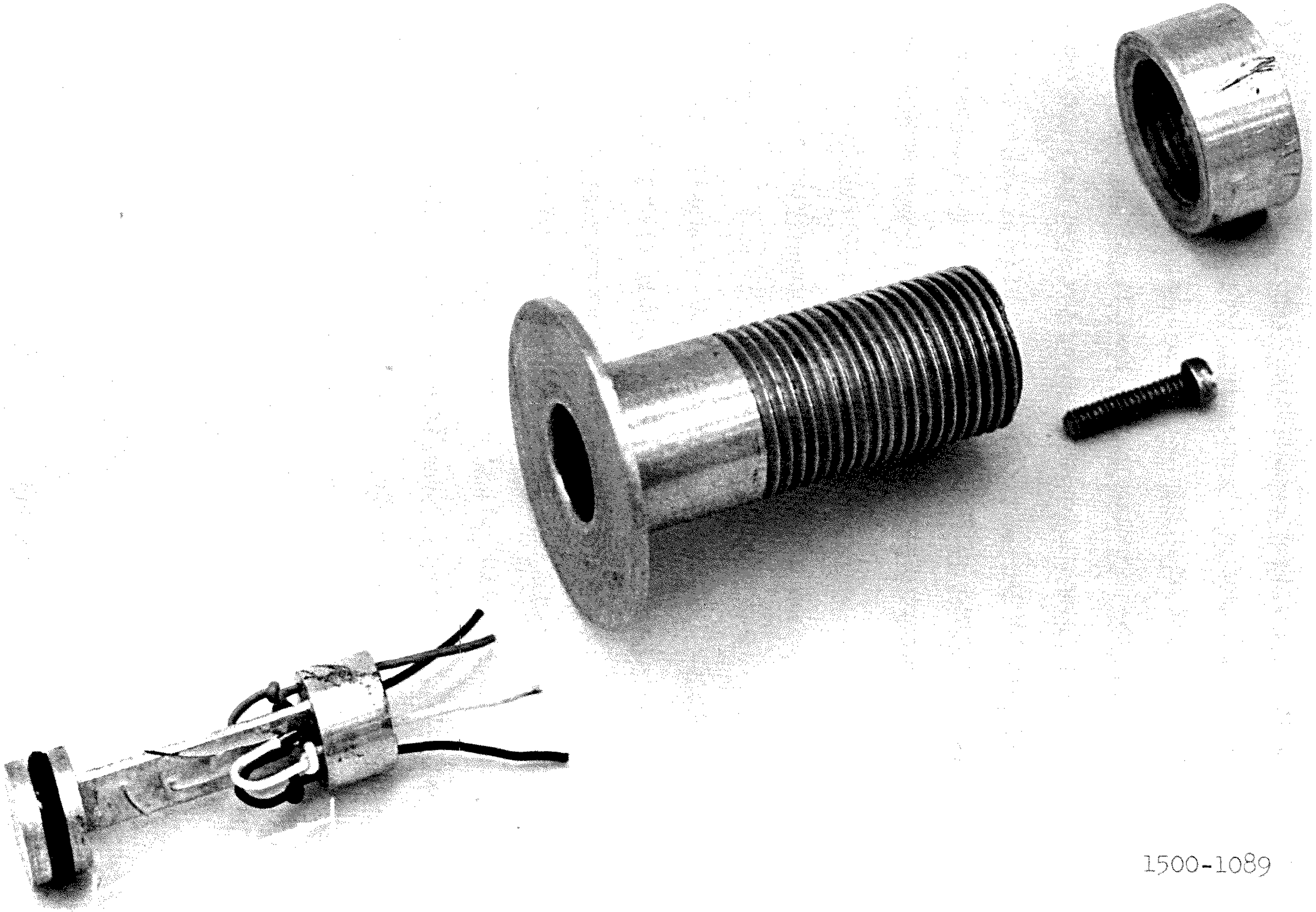

Fig. 1. On-structure soil stress gage

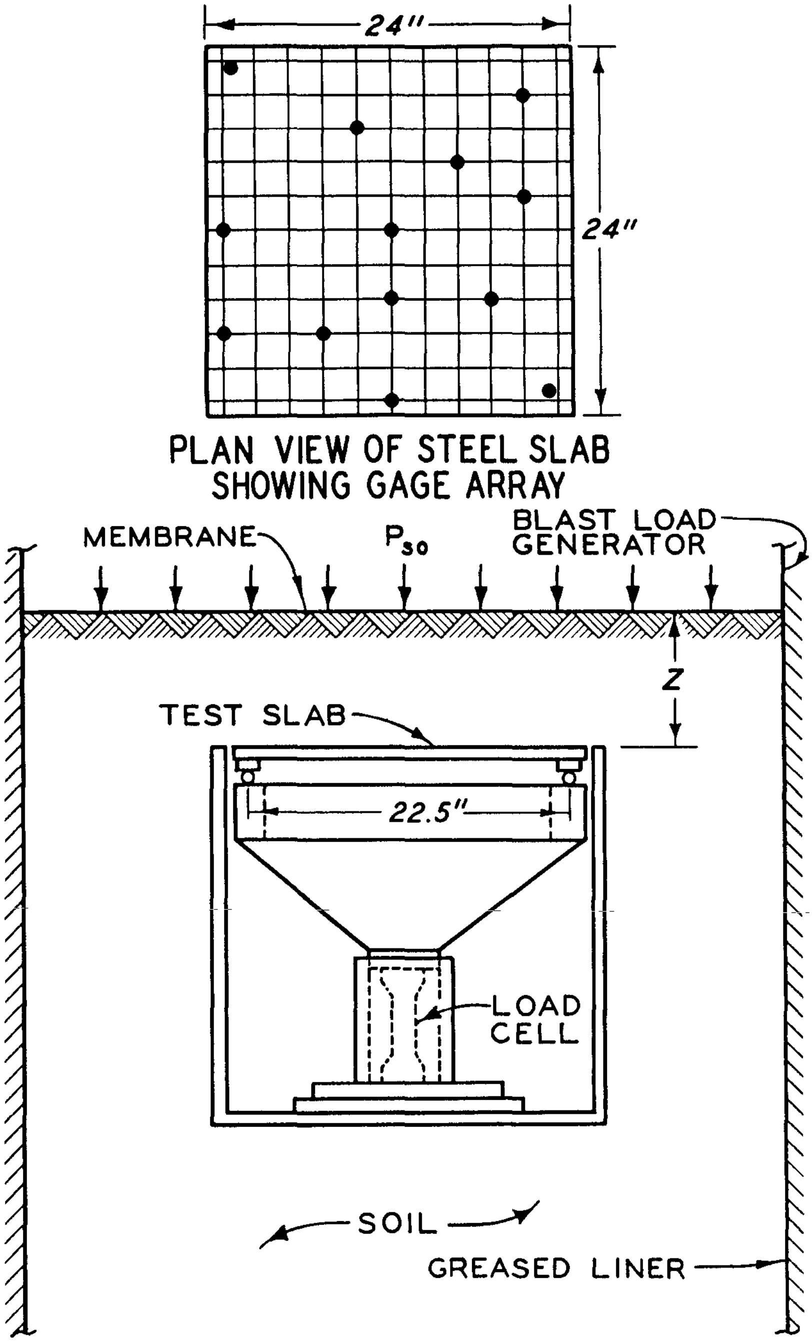

Fig. 2. Gage array and test geometry

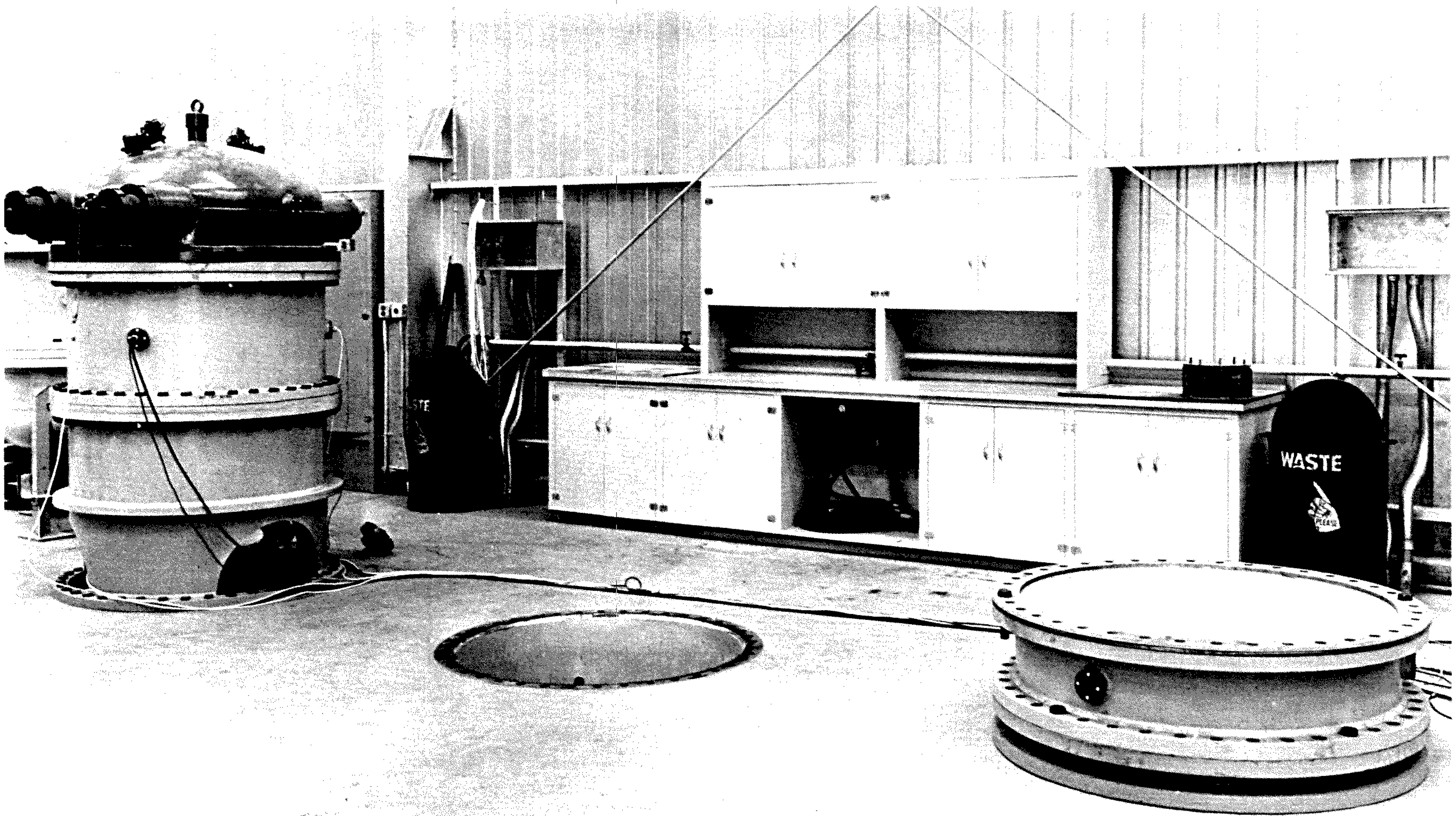

1500-1225

Fig. 3. Small Blast Load Generator facility

comprehensive description of the facility is given by Albritton (1).

The 9.5-ft soil column formed the base for the tests conducted in this study. The test assembly rested on a 1-ft layer of sand over the floor level. The necessary number of rings were stacked to build up the cover. To minimize sidewall friction effects, a greased liner[3] was provided from the soil surface to the floor level. In addition, a membrane was provided over the soil surface to prevent air pressure from penetrating the voids. In all cases, the depth of burial was measured from the bottom of the membrane to the top of the plate. During the dynamic shots, a 1/2-in. loose cover of sand protected the membrane from the heat generated by the explosion.

The soil density was controlled from 1 ft below the base of the box by showering the sand from a predetermined height. The soil sample was rebuilt for each test.

The soil used in the tests is known as Cook's Bayou sand. It is a uniform, fine sand with only a negligible percentage finer than the No. 200 sieve. Its maximum and minimum dry unit weights are 110.8 and 93.3 pcf, respectively. The angle of friction increases from 34.5° to 42.0° as the dry unit weight increases from 98.5 to 109.0 pcf. Durbin (3) and Kennedy et al. (6) give information on the properties and stress-strain characteristics of this sand.

The static and airblast overpressures were measured by a commercially available strain gage-type pressure transducer screwed into the bonnet of

---

[3]Described by P. F. Hadala in "Sidewall Friction Reduction in Static and Dynamic Small Blast Load Generator Tests," U. S. Army Engineer Waterways Experiment Station, Vicksburg, Miss. (in preparation).

the SBLG. Fig. 3 shows a pressure transducer mounted between the two firing tubes. The plate deflections relative to the supports were measured by a linear variable differential transformer. Light beam galvanometer oscillographs with a frequency response of 1000 cps and paper speed of 160 ips were used in the dynamic tests to record the amplified output for the data channels used in this study.

The static tests were conducted by applying air pressure in increments of approximately 10 psi during loading and decreasing by approximately 20 psi during unloading. Dynamic tests were conducted in the SBLG by detonating explosives in the firing tubes which are surrounded by baffles to create an airblast shock that produces a uniform pressure over the soil surface. Zero time is recorded when the explosive is detonated and indicated on all records by a discontinuity in the time trace.

SURFACE FIT

The stress at the soil-structure surface is approximated mathematically by a polynomial of the form

$$q(x,y) = \sum_{i,j=0}^{3} a_{ij} x^i y^j \tag{1}$$

It is assumed that the surface is symmetrical and the n experimental data points can be collapsed to one octant of the square plate, making the coefficients a_{ij} equal to a_{ji}. It is also assumed that the slope of the surface at the center of the plate is zero, so that

$$\left(\frac{\partial q}{\partial x}\right)_{x=0} = \left(\frac{\partial q}{\partial y}\right)_{y=0} = 0 \tag{2}$$

Eq. 2 can be satisfied if

$$a_{1j} = a_{i1} = 0 \tag{3}$$

These conditions reduce the number of coefficients in Eq. 1 from sixteen to six. The equation can be written as

$$q(x,y) = a_{00} + a_{02}(x^2 + y^2) + a_{03}(x^3 + y^3)$$

$$+ a_{22}\, x^2y^2 + a_{23}\, x^2y^2(x + y)$$

$$+ a_{33}\, x^3y^3 \tag{4}$$

Eq. 4 can be expressed as

$$q(x,y) = a_1X_1 + a_2X_2 + a_3X_3 + a_4X_4 + a_5X_5 + a_6X_6$$

where

$$X_1 = 1 \ ,\ X_2 = (x^2 + y^2),\ X_3 = (x^3 + y^3)$$

$$X_4 = x^2y^2 \ ,\ X_5 = x^2y^2(x + y),\ X_6 = x^3y^3 \tag{5}$$

and the corresponding coefficients are replaced by a_1 , a_2 ,...a_6 .

The coefficients can be determined by solving the six normal equations obtained by the least squares method (see Natrella (10)).

$$a_1 \sum_{k=1}^{n} X_{1k}^2 + a_2 \sum_{k=1}^{n} X_{1k}X_{2k} + \ldots + a_6 \sum_{k=1}^{n} X_{1k}X_{6k} = \sum_{k=1}^{n} X_{1k}Q_k$$

$$a_1 \sum_{k=1}^{n} X_{2k}X_{1k} + a_2 \sum_{k=1}^{n} X_{2k}^2 + \ldots + a_6 \sum_{k=1}^{n} X_{1k}X_{6k} = \sum_{k=1}^{n} X_{2k}Q_k \qquad (6)$$

$$\cdot \quad \cdot \quad \cdot \quad \cdot \quad \cdot \quad \cdot \quad \cdot$$

$$a_1 \sum_{k=1}^{n} X_{61}X_{1k} + a_2 \sum_{k=1}^{n} X_{6k}X_{2k} + \ldots + a_6 \sum_{k=1}^{n} X_{6k}^2 = \sum_{k=1}^{n} X_{6k}Q_k$$

The X's are determined exactly by the location of the 13 soil-stress gages, and the Q's are experimental values obtained from soil-stress measurements.

PRESENTATION OF RESULTS

The data from the 13 soil-stress gages, the load cell, and the overpressure gage were input into a computer program which solved for the six coefficients and computed values of soil stress (the terms soil-stress distribution and pressure distribution are used interchangeably) at locations on a 5 by 5 grid of one quadrant of the plate. The total load on the plate was computed by evaluating the integral

$$\int_A q(x,y)\ dA \qquad (7)$$

The six coefficients are input to another program which outputs the oblique projection plots displayed in this paper. The plots are non-dimensionalized by dividing the soil stress by the overpressure and the x and y direction by the quadrant length. The quadrant length is one-half the distance between supports, the distance between the supports being 22.5 in. and the overall length being 24 in. The integration of Eq. 7 is carried out for a length of 24 in.

RESULTS AND DISCUSSION

Static Tests.--A zero depth of burial (no soil cover) static test was conducted for the purpose of correlating the values obtained from the bonnet gage that measured the overpressure in the test chamber, the soil-stress gages that measured stress on the plate, and the load cell that measured the total load applied to the slab. The following values summarize the results at one pressure level:

Bonnet Pressure psi	Soil Stress, psi Mean Value	Soil Stress, psi Standard Deviation	Load Cell kips
44.89	49.34	4.77	25.48

The total load on the plate calculated from the bonnet pressure is 25.89 kips, which is less than 2 percent different from the load-cell reading. The higher values for the soil-stress gages are probably caused by errors introduced by the nonlinear calibration associated with this gage for relatively low outputs of the magnitude recorded for this test.

The results of the 12-in. depth of burial static test are shown at surface overpressure (p_{so}) intervals of approximately 10 psi for the load cycle and 20 psi for the unload cycle in Figs. 4 and 5, wherein the experimental data are compared to the values computed from the surface fit at gage locations collapsed to one octant of the plate. The duplicate gages at two locations show maximum variations in stress of approximately 10 percent except at the first pressure level of 8.3 psi. The deviations from the

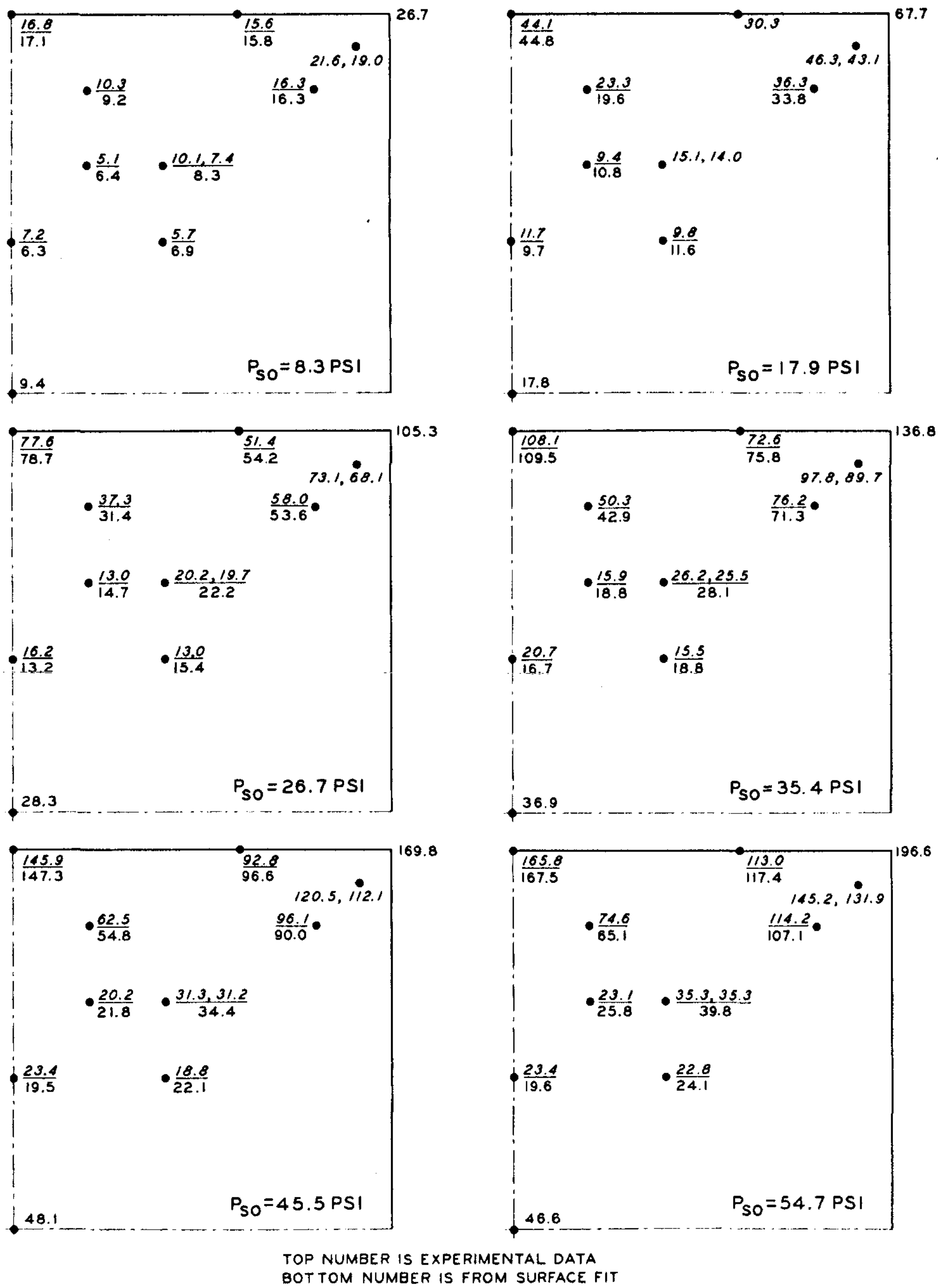

Fig. 4. Experimental soil-stress data and surface fit values for static test (load cycle) at 12-in. depth of burial

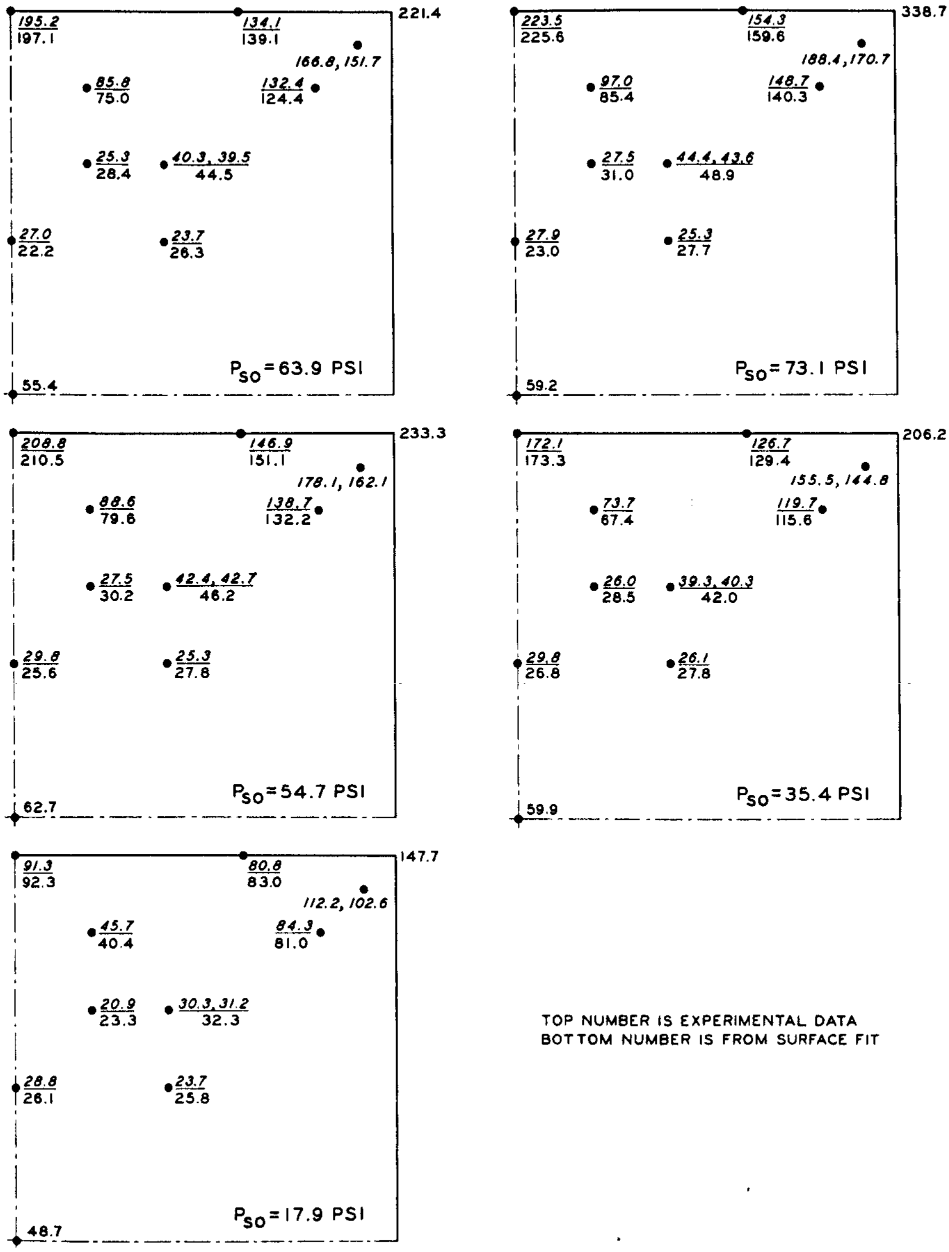

Fig. 5. Experimental soil-stress data and surface fit values for static test (part of load, and unload cycle) at 12-in. depth of burial

third order, fitted surface are considered reasonable. The gage at the center of the plate malfunctioned and the surface remains unchecked except for the imposed zero slope condition at the origin.

Shown in Figs. 6 through 16 are nondimensional plots of pressure distribution on one quadrant of the plate. The plots are almost identical for the load cycle, but during unloading the ratio of soil stress to overpressure increased to more than double the corresponding values of the load cycle. Comparisons of load and unload distribution can be made at surface pressures of 54.7, 35.4, and 17.9 psi. The reason for the stress magnification on unload is probably due to the stiff soil-stress gage pushing into the partially locked soil mass. McNulty's (8) study of arching in sand shows that very small structural deflections cause significant changes in load. The dependence of the total load on the plate on the deflection of the plate is illustrated in Figs. 17a and b. The total load on the plate during the load cycle is approximately 1.4 times the total reaction. During the unload cycle the ratio increases to 1.78. The discrepancy between the total load on the plate and the reaction is probably due to the difference in the deformation characteristics of the soil-stress gage, the plate, load collector, and load cell. The need for improved on-structure soil-stress measurements is evident from these plots. Assuming that the load cell measuring the reaction accurately represents the total load on the plate a correction to the surface can be made by altering the coefficients by a constant multiplier so that the total load on the plate equals the total reaction. The variations of the six coefficients with surface overpressure are shown in Fig. 18. The kink in the curve occurring at pressures between 45 and 55 is probably attributable to the increasing stiffness of the

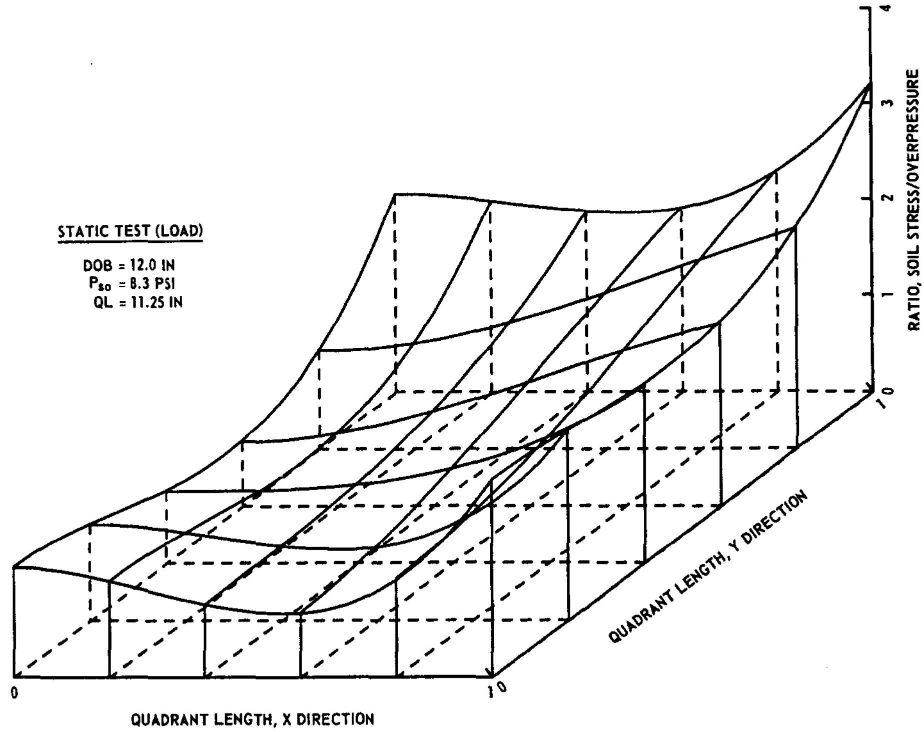

Fig. 6. Soil-stress distribution across one quadrant of plate for static surface overpressure of 8.3 psi

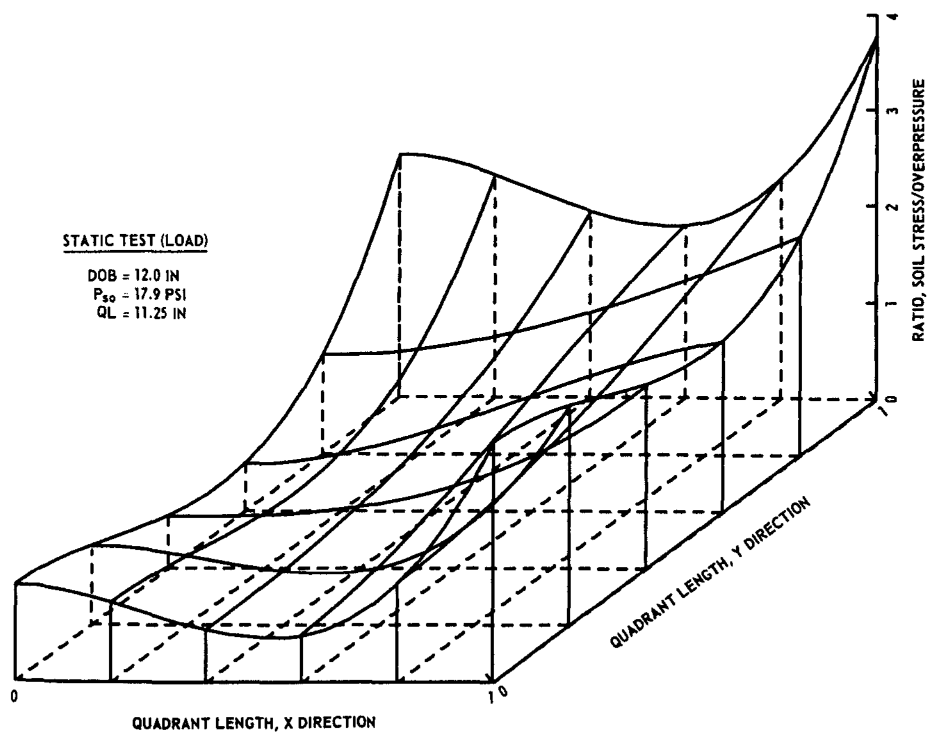

Fig. 7. Soil-stress distribution across one quadrant of plate for static surface overpressure of 17.9 psi

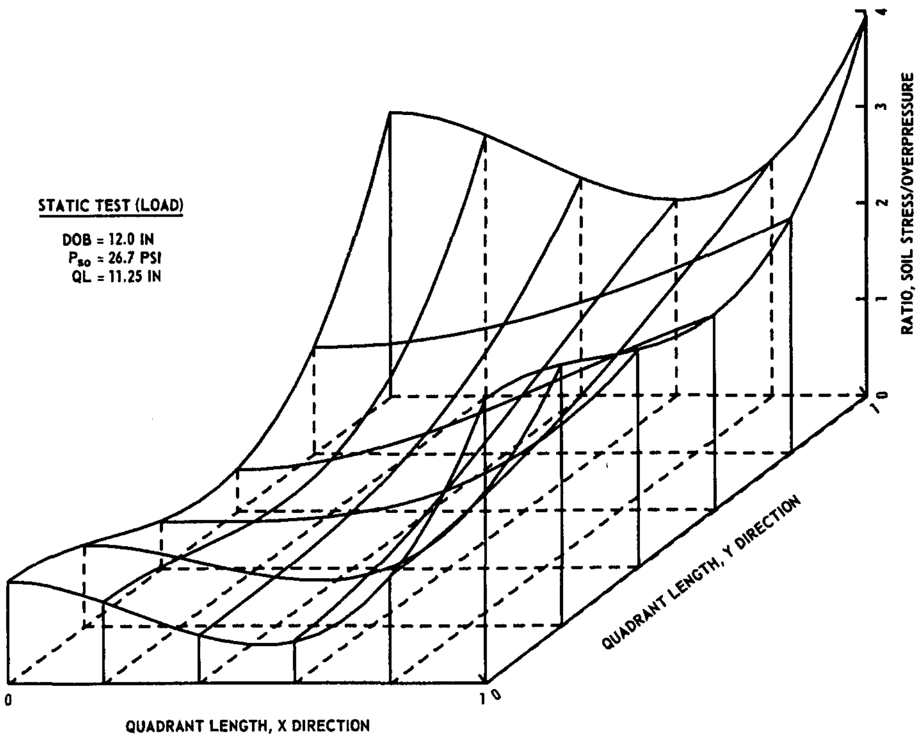

Fig. 8. Soil-stress distribution across one quadrant of plate for static surface overpressure of 26.7 psi

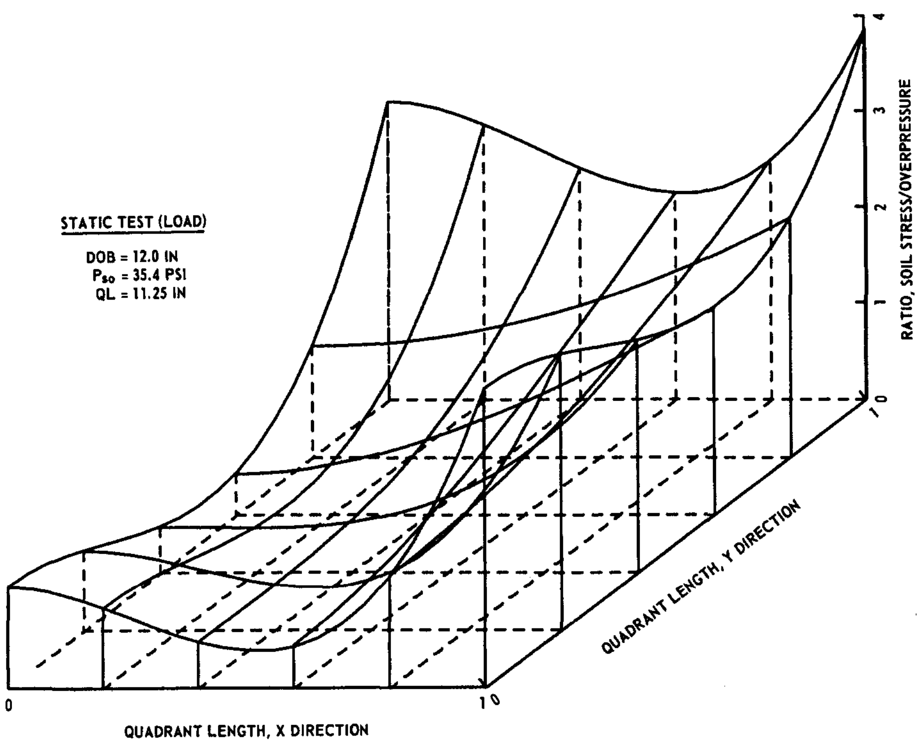

Fig. 9. Soil-stress distribution across one quadrant of plate for static surface overpressure of 35.4 psi

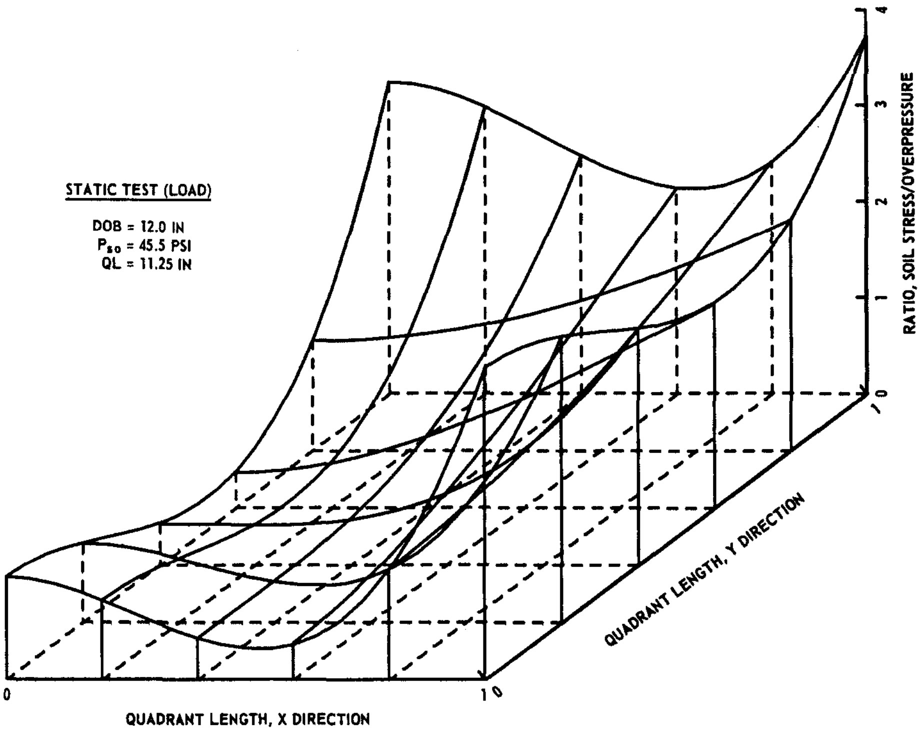

Fig. 10. Soil-stress distribution across one quadrant of plate for static surface overpressure of 45.5 psi

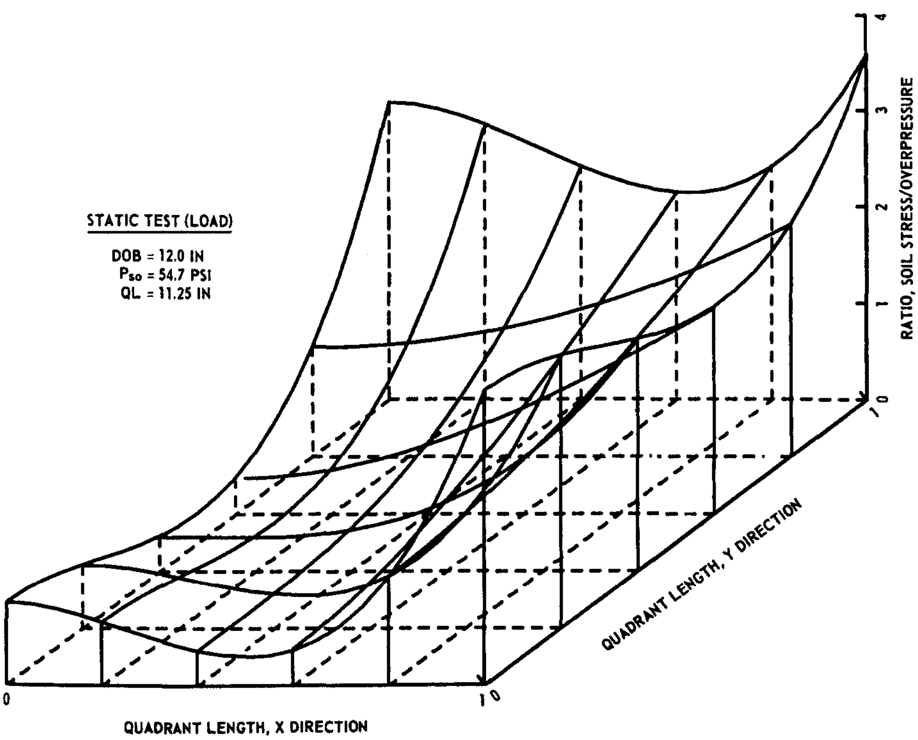

Fig. 11. Soil-stress distribution across one quadrant of plate for static surface overpressure of 54.7 psi

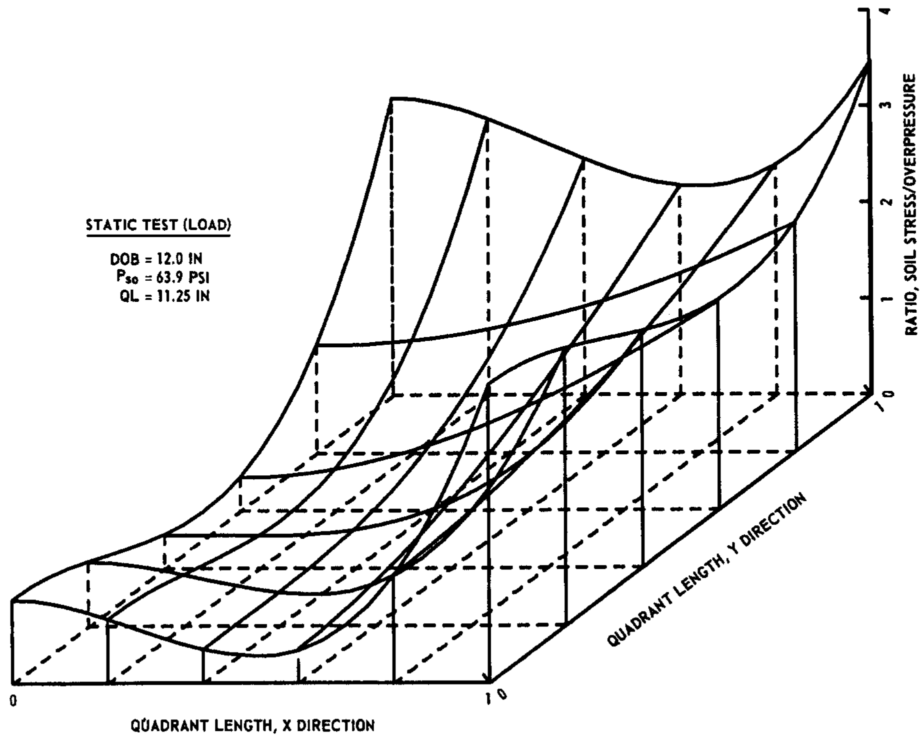

Fig. 12. Soil-stress distribution across one quadrant of plate for static surface overpressure of 63.9 psi

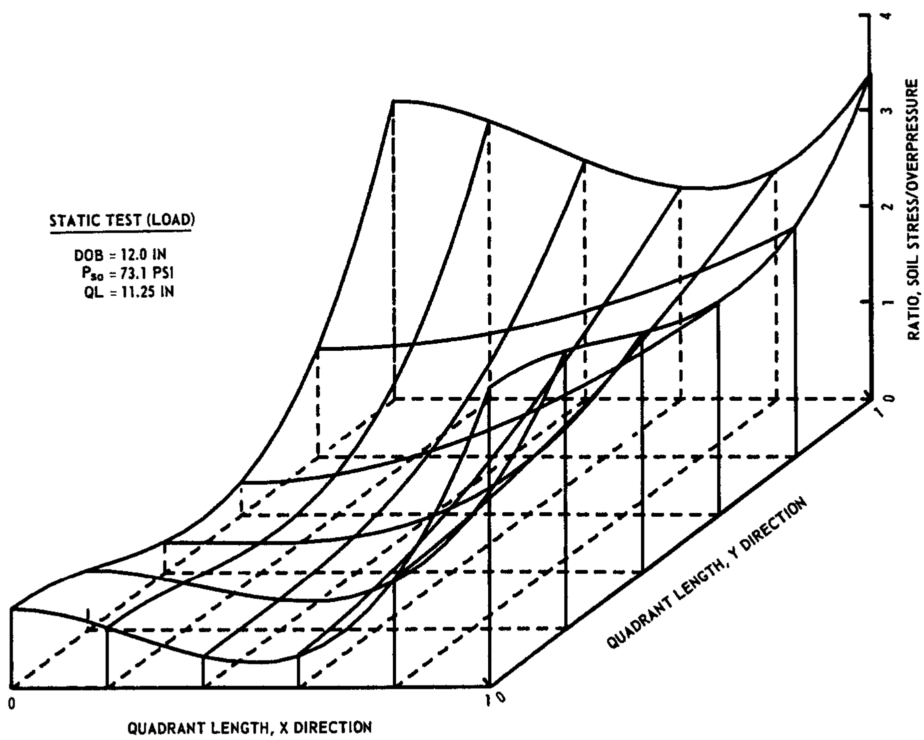

Fig. 13. Soil-stress distribution across one quadrant of plate for static surface overpressure of 73.1 psi

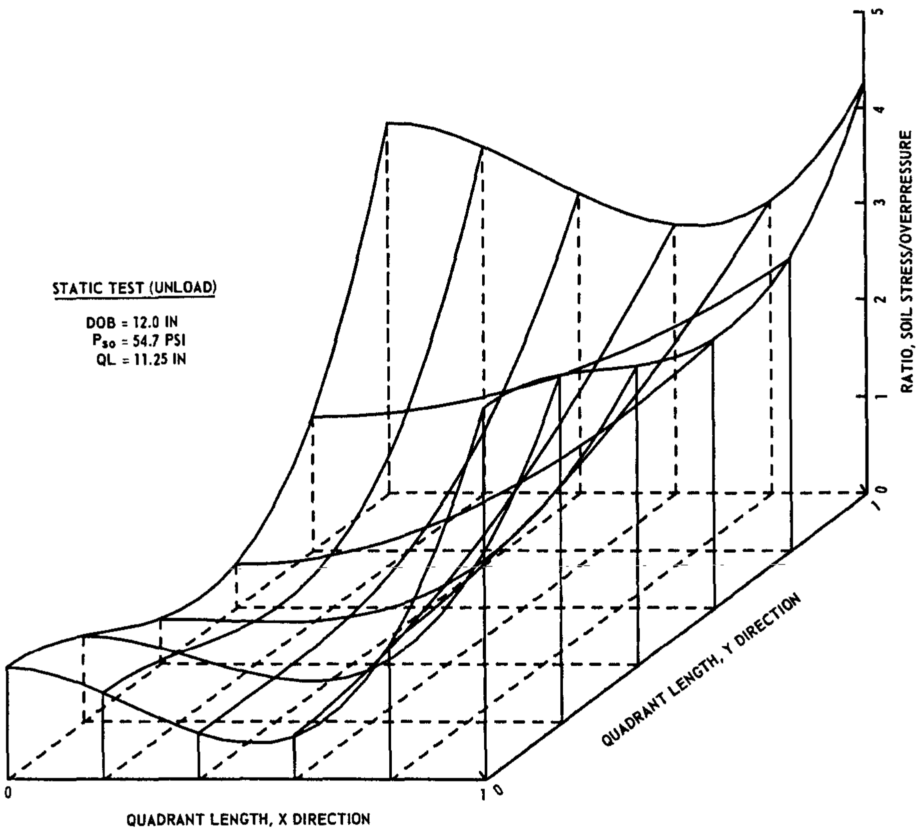

Fig. 14. Soil-stress distribution across one quadrant of plate for static surface overpressure of 54.7 psi

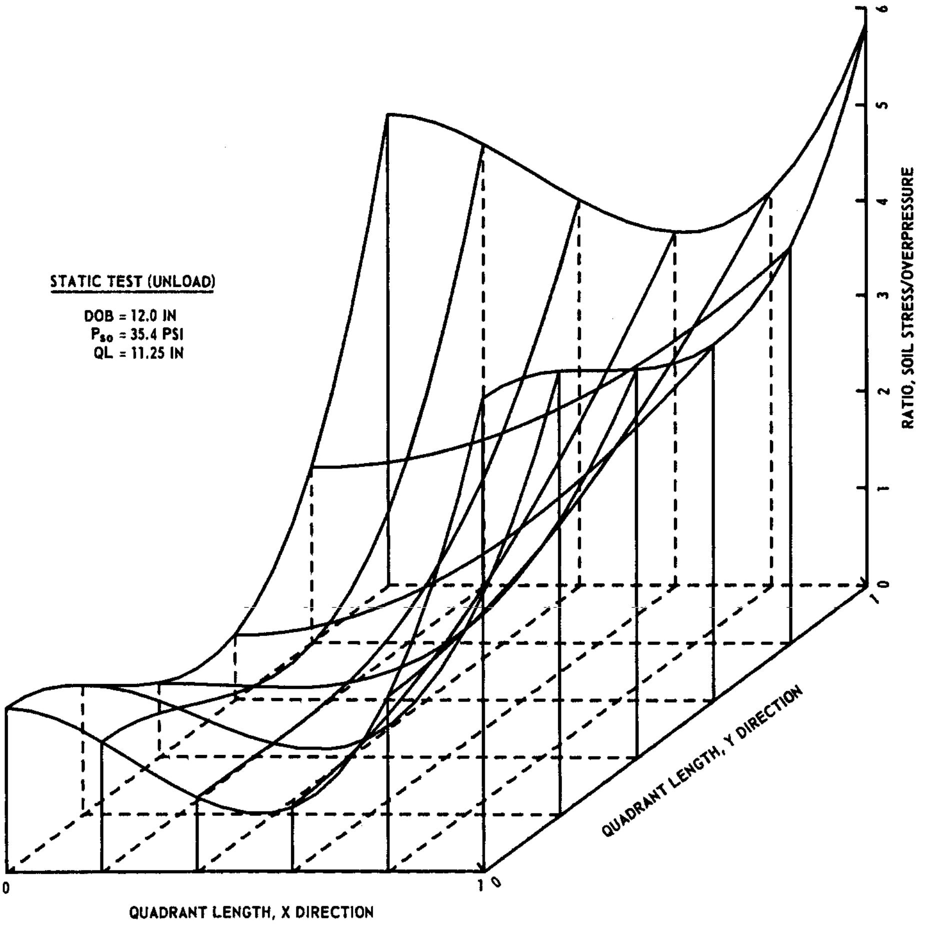

Fig. 15. Soil-stress distribution across one quadrant of plate for static surface overpressure of 35.4 psi

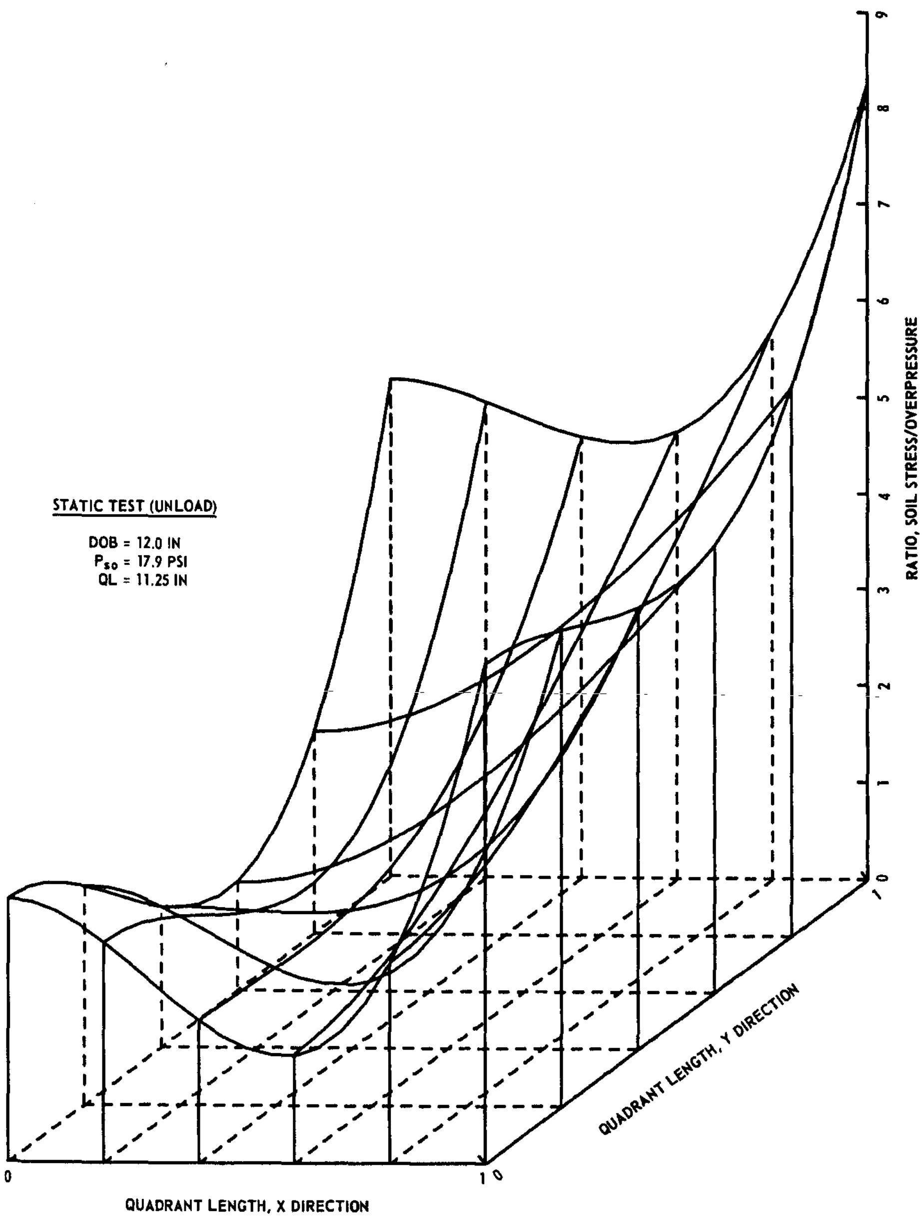

Fig. 16. Soil-stress distribution across one quadrant of plate for static surface overpressure of 17.9 psi

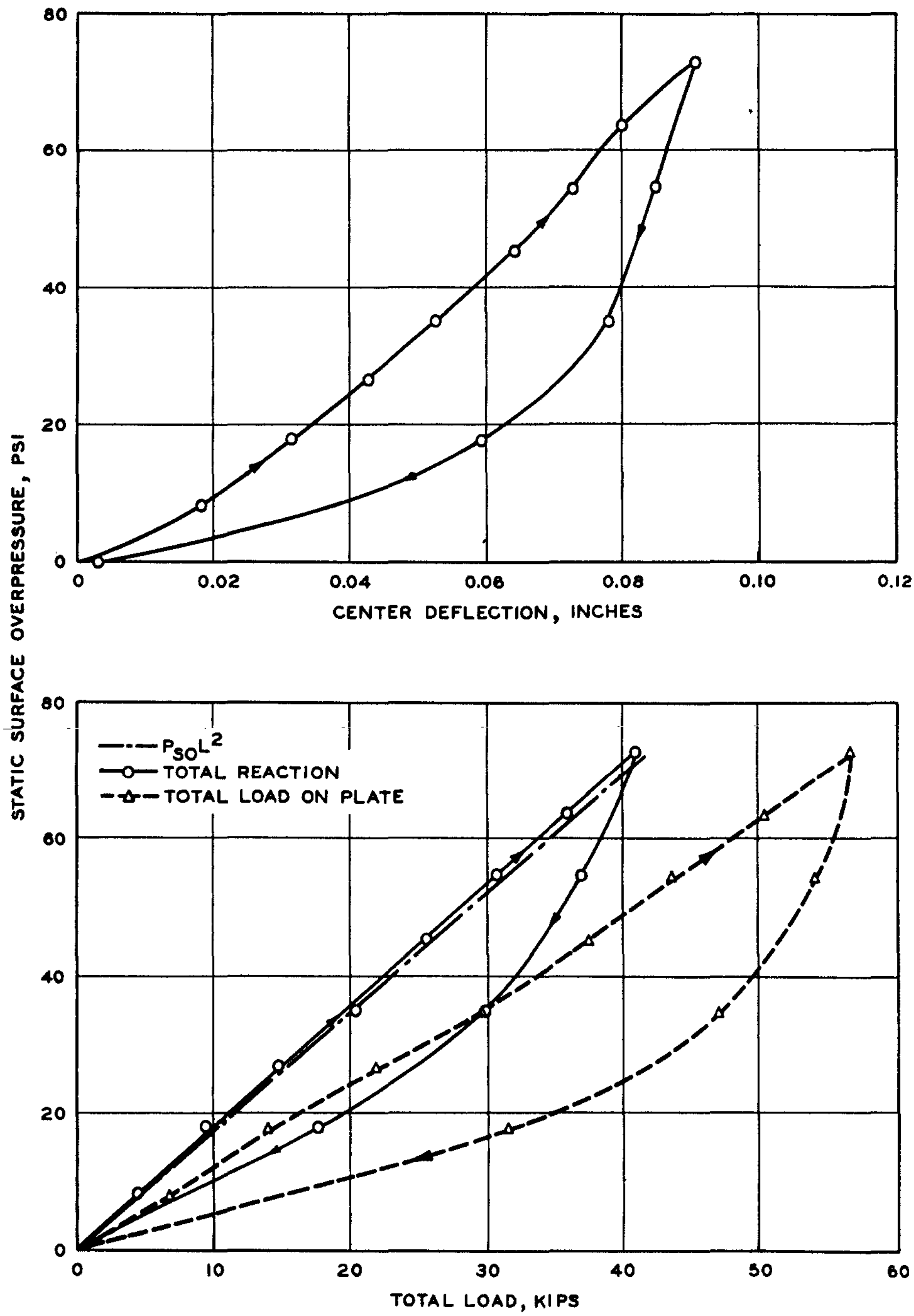

Fig. 17. Center deflection and total load for static test

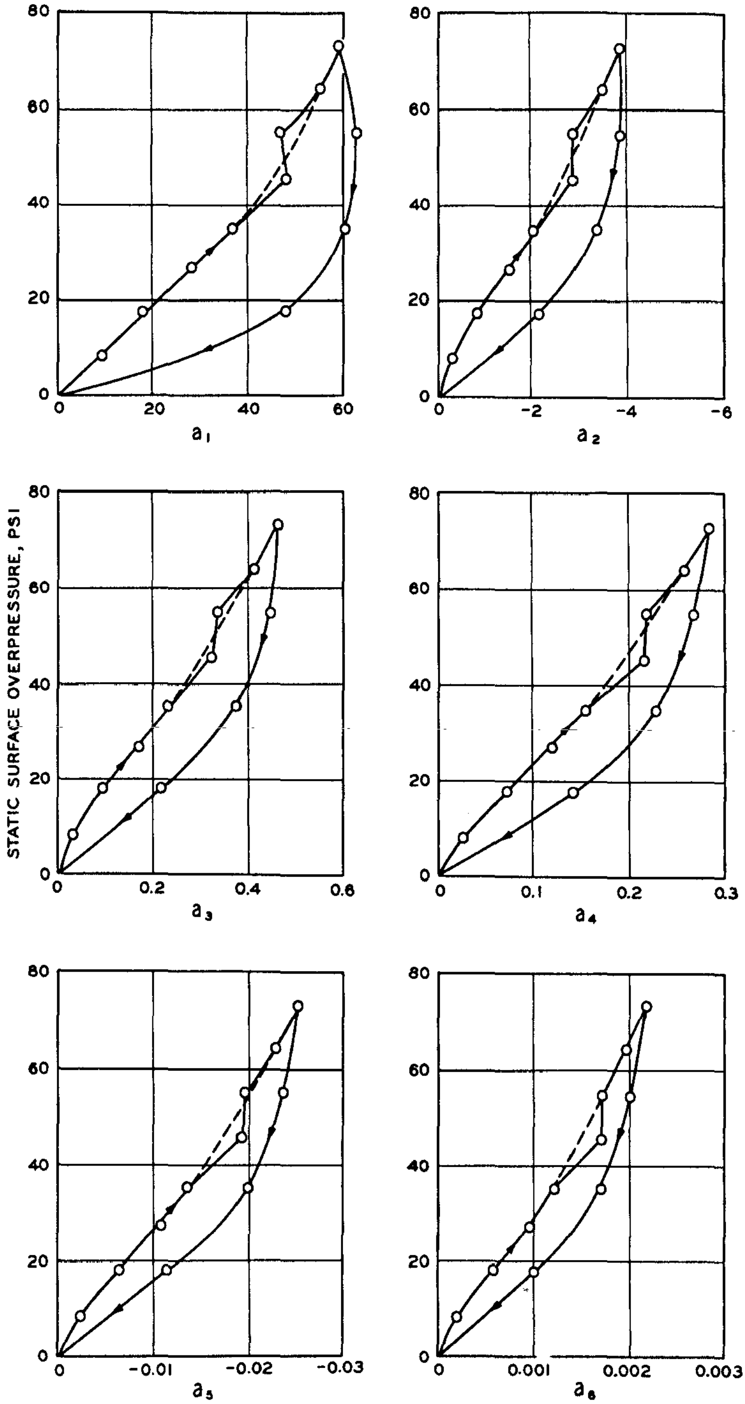

Fig. 18. Variation of coefficients with static surface overpressure

sand or to an inflection in the stress-strain characteristics at this pressure level.

Dynamic Tests.--The results of the dynamic test at zero depth of burial are shown in Fig. 19. For the zero depth of burial there is in reality a 1/2-in. soil cover over the membrane, as explained earlier in the description of the experimental procedure. The airblast overpressure (shown by dashed line on airblast overpressure-time trace) was 54 psi. The soil-stress gages on the plate registered values ranging from 61.9 psi at the center to 83.6 psi near the corner. The overregistration is probably caused by the 1/2-in. layer of sand over the plate. The total reaction measured by the load cell includes the inertial effect of the plate and the load collector. As the motion diminishes, the total load on the plate should equal the value recorded for the load cell but, as in the static case, the total load on the plate is higher. A comparison of $P_{so}L^2$ with the load-cell reading indicates more load transferred to the plate in the dynamic case than in the static case where the two were nearly equal during the loading cycle.

The experimental results and the surface fit values for the first dynamic shot at a 12-in. depth of burial are shown in Fig. 20. The ratio of the load on the plate to the reaction varies from 1.14 at 8.1 msec to 1.67 at 30 msec.

Shown in Figs. 21 through 24 are the stress distribution plots at four different times. A significantly different characteristic of these plots is the decreasing stress distribution at the corner. Mason et al. (7) measured stress distributions on a 6-in.-diam right circular cylinder at varying depths for dynamic input pressures. Below a critical depth, the stress distribution was greater than the free-field stress at the center of

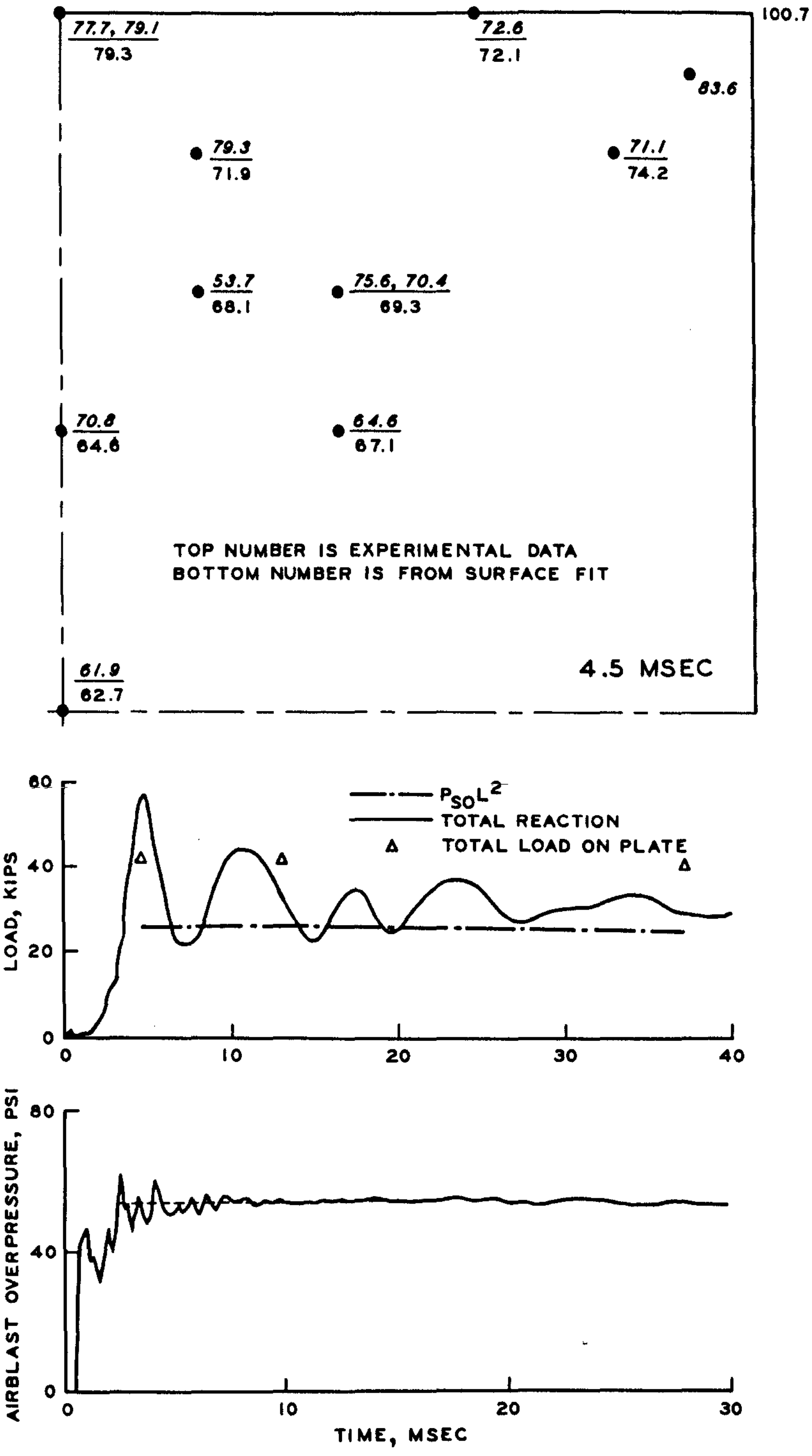

Fig. 19. Experimental data and surface fit values for dynamic test at zero depth of burial

69583

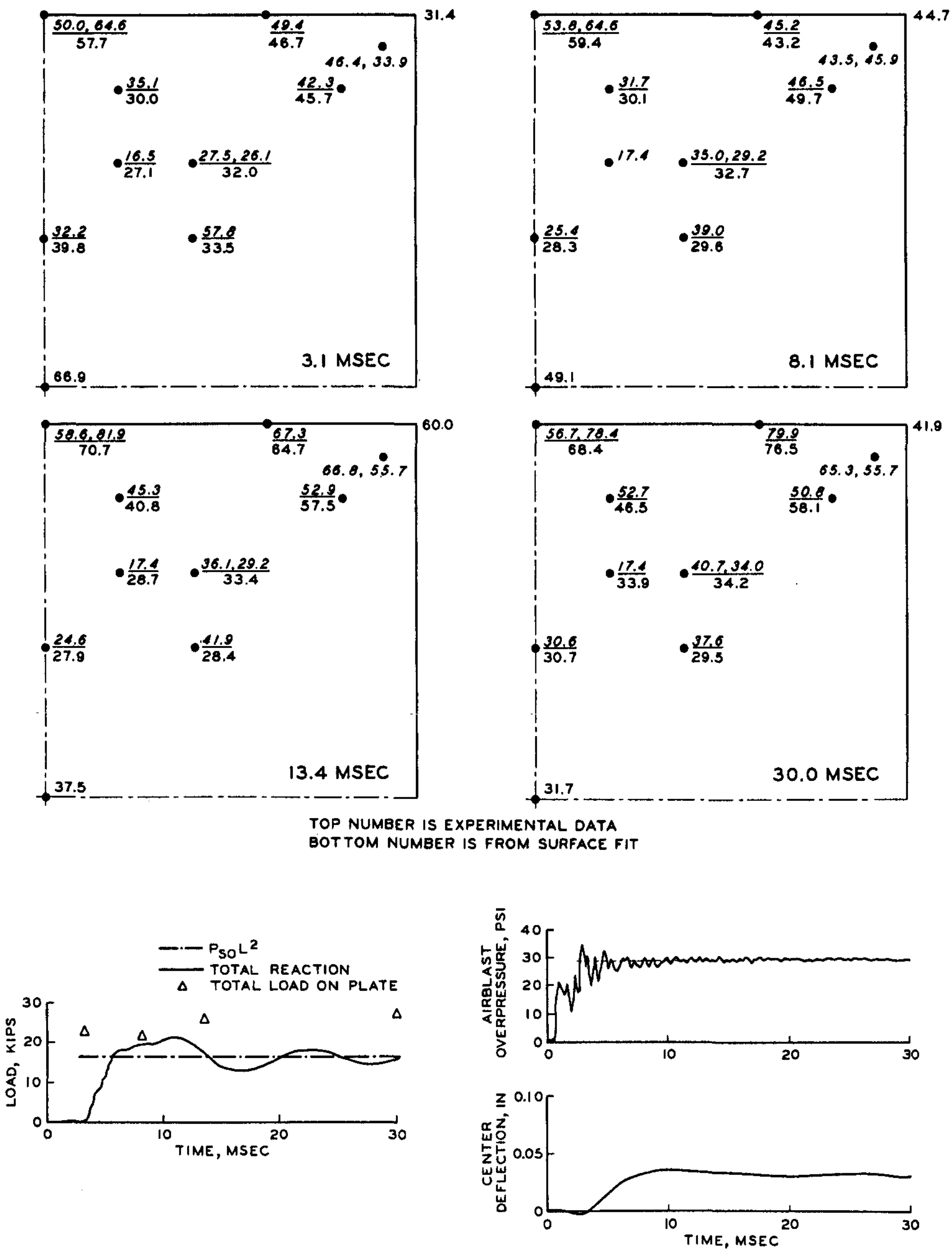

Fig. 20. Experimental data and surface fit values for dynamic test 1 at 12-in. depth of burial

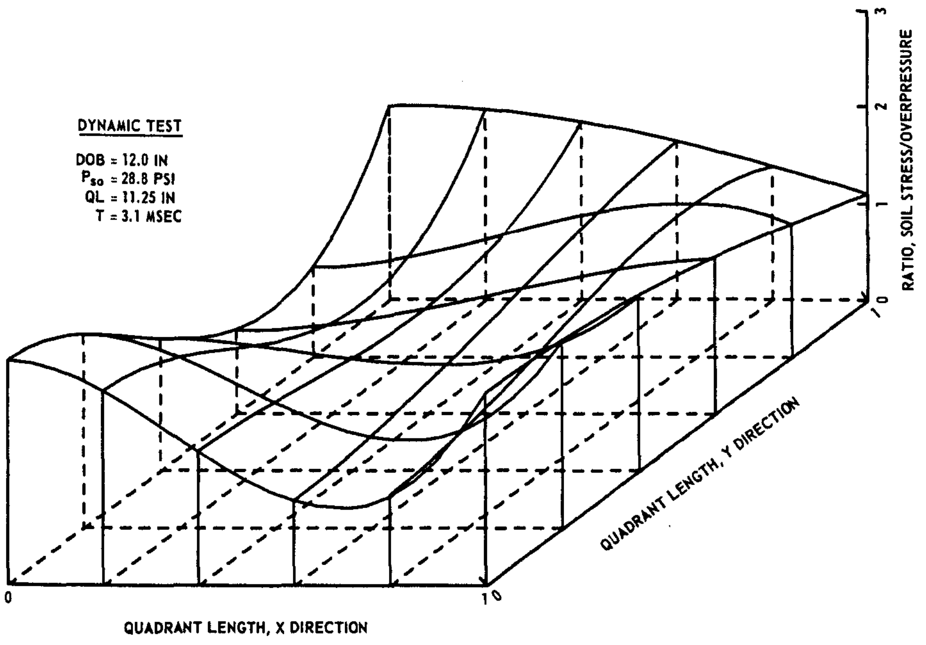

Fig. 21. Soil-stress distribution across one quadrant of plate for dynamic test 1 at 3.1 msec

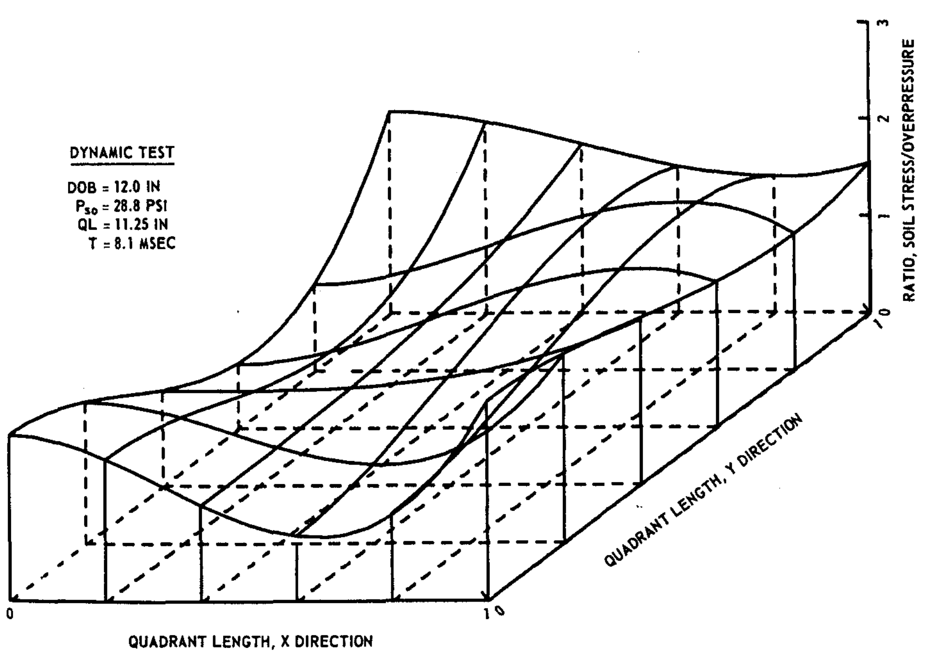

Fig. 22. Soil-stress distribution across one quadrant of plate for dynamic test 1 at 8.1 msec

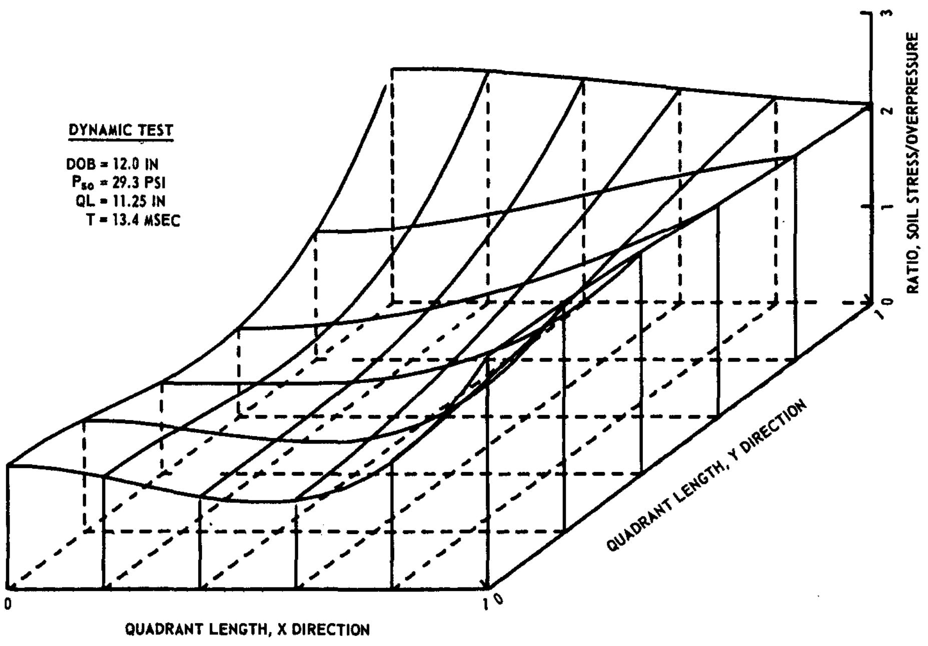

Fig. 23. Soil-stress distribution across one quadrant of plate for dynamic test 1 at 13.4 msec

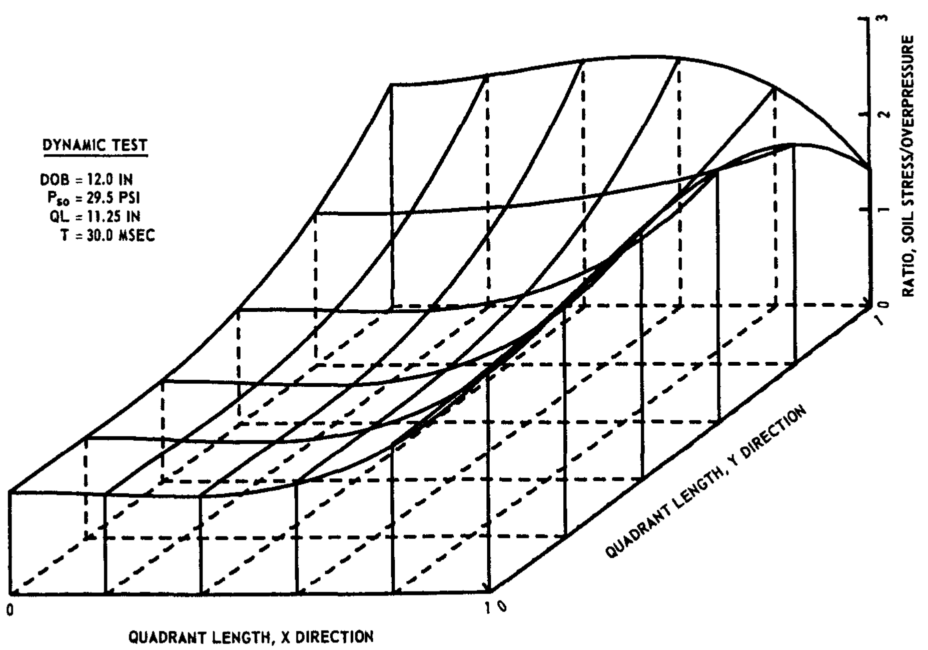

Fig. 24. Soil-stress distribution across one quadrant of plate for dynamic test 1 at 30.0 msec

the structure and decreased to a value lower than free field at the edge. Above the critical depth, they found the stress distribution varying from slightly above free field at the center to larger values at the edge.

The experimental data, surface fit values, and stress distribution for the second and third dynamic shots at a 12-in. depth of burial are shown in Figs. 25 through 36. The distributions, which are similar for both dynamic shots, increase in magnitude for times up to 12 msec after zero time. The deflection of the center of the plate reaches a maximum value at 15 msec after zero time. The rate at which the displacement of the plate changes seems to influence the rate at which the values of stress increase for the soil-stress gages located on the plate.

CONCLUSIONS

The following conclusions are based on one depth of burial in dry sand and a limited pressure range.

1. The ratio of the static soil stress to overpressure is higher during the unload cycle than during the load cycle. The ratio remains relatively constant during the load cycle and increases during the unload cycle.

2. The dynamic soil-stress distribution varies with overpressure and time. Above a certain overpressure level, the distribution and variation with time essentially remain the same.

3. The overregistration of the total load on the plate, determined from the pressure surface fit utilizing values obtained from the on-structure soil-stress gages, compared to the reaction measured by the single load cell was considerably greater for both the static and dynamic tests at times

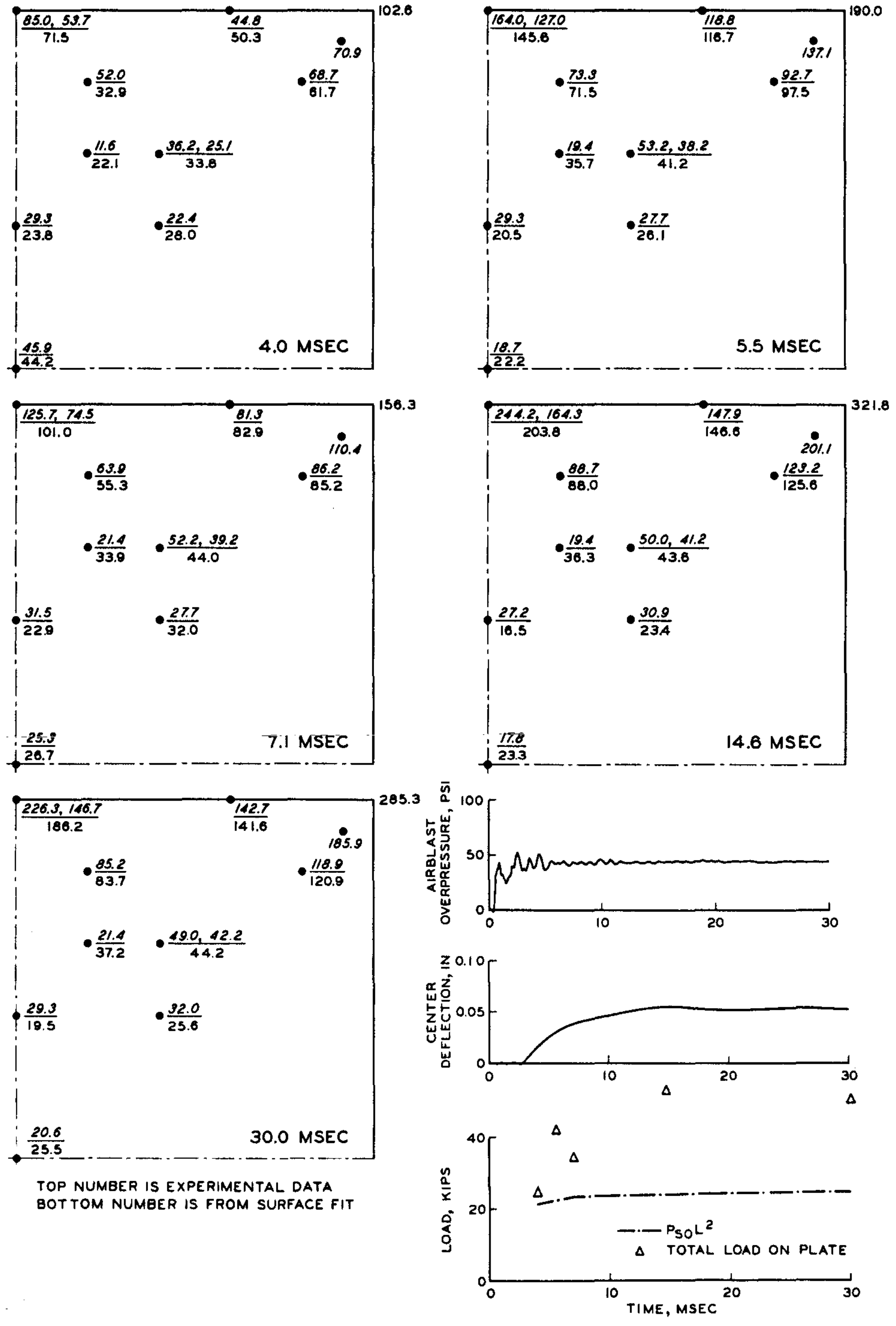

Fig. 25. Experimental data and surface fit values for dynamic test 2 at 12-in. depth of burial

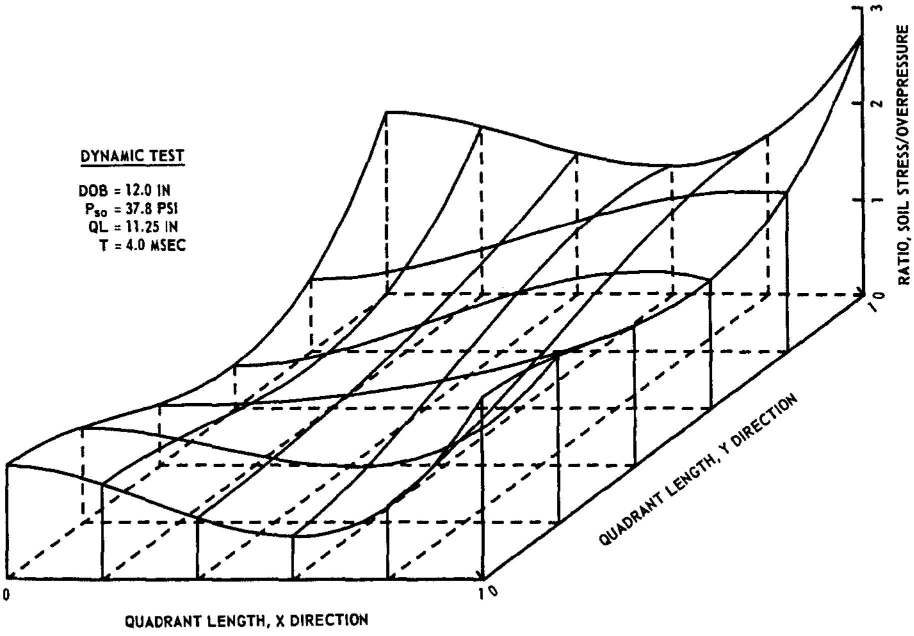

Fig. 26. Soil-stress distribution across one quadrant of plate for dynamic test 2 at 4.0 msec

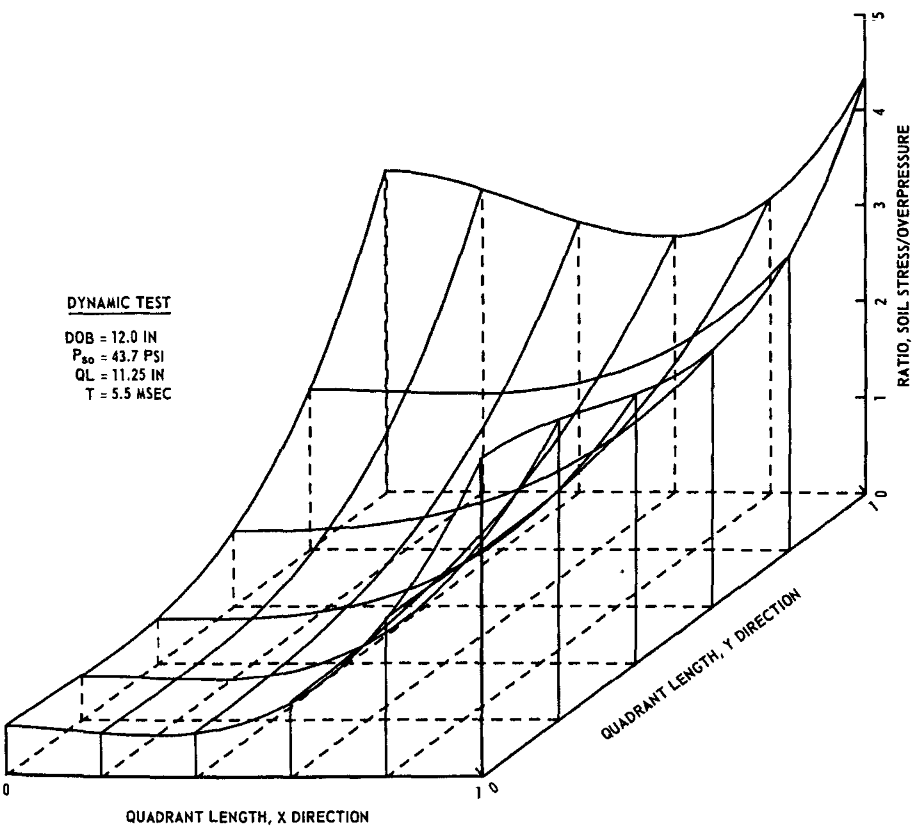

Fig. 27. Soil-stress distribution across one quadrant of plate for dynamic test 2 at 5.5 msec

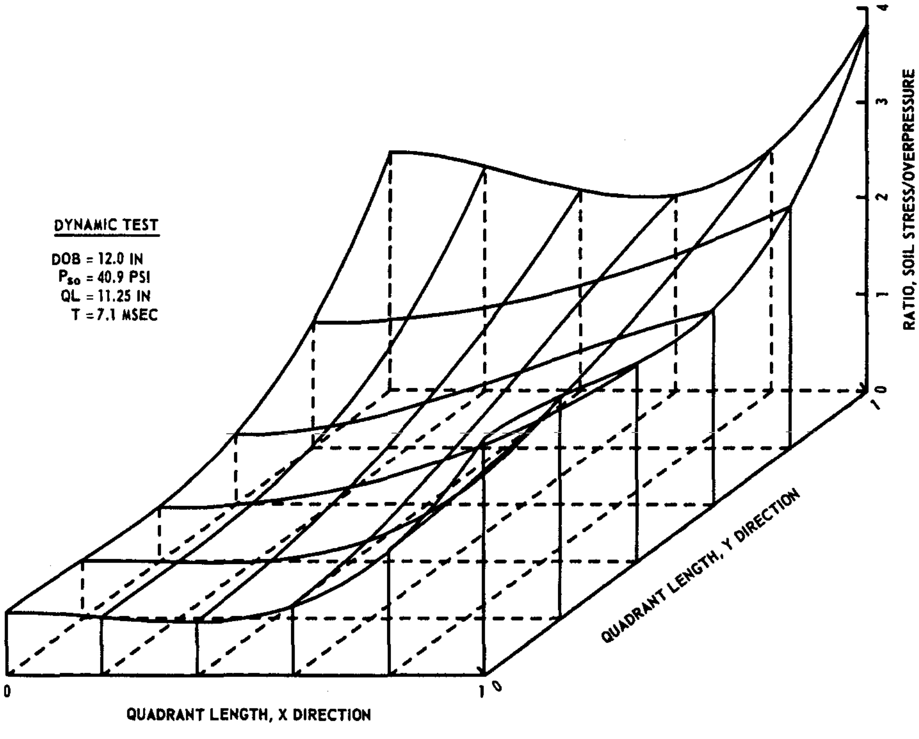

Fig. 28. Soil-stress distribution across one quadrant of plate for dynamic test 2 at 7.1 msec

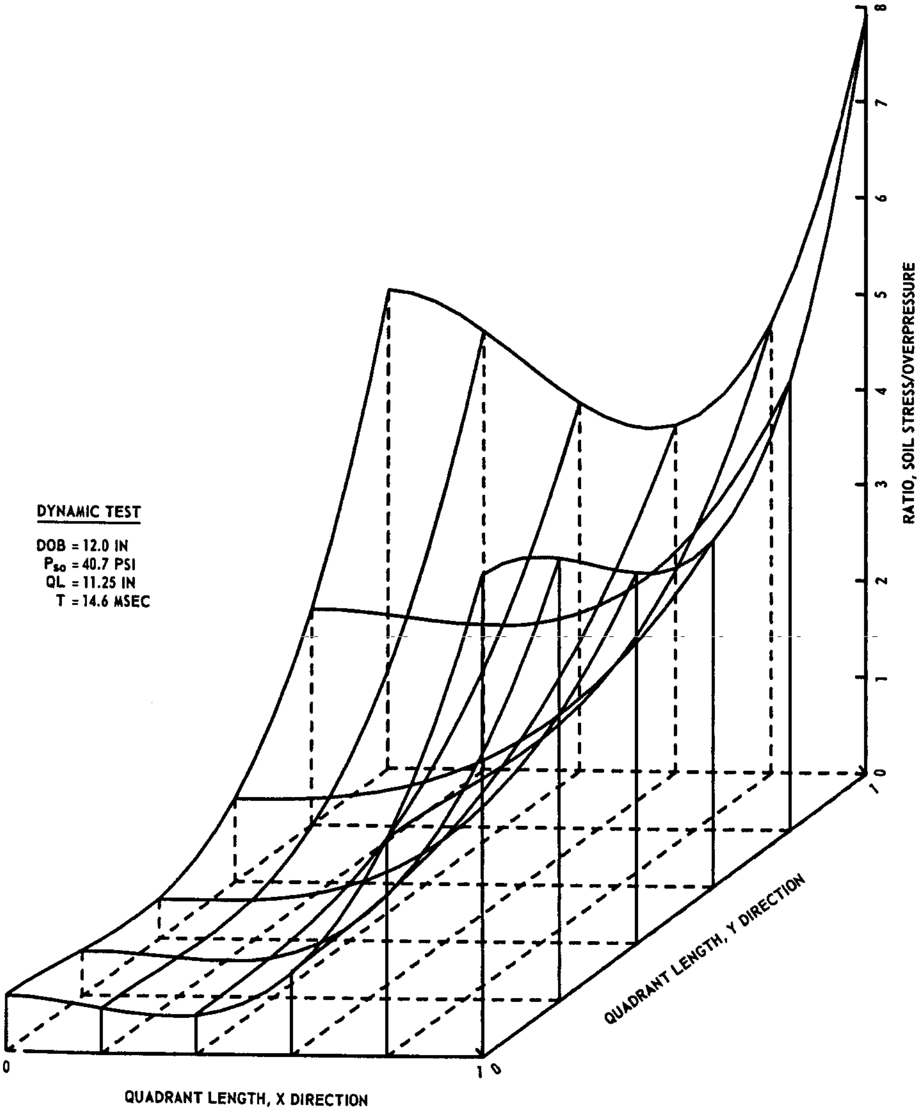

Fig. 29. Soil-stress distribution across one quadrant of plate for dynamic test 2 at 14.6 msec

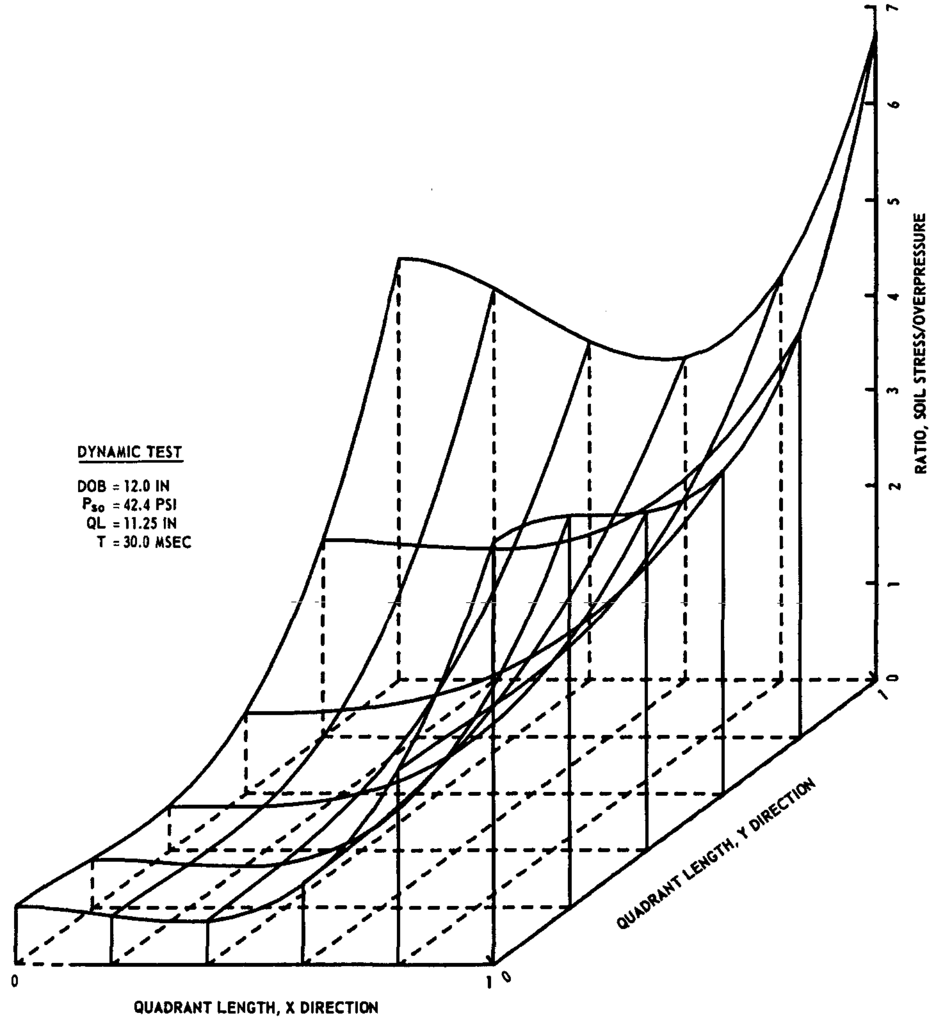

Fig. 30. Soil-stress distribution across one quadrant of plate for dynamic test 2 at 30.0 msec

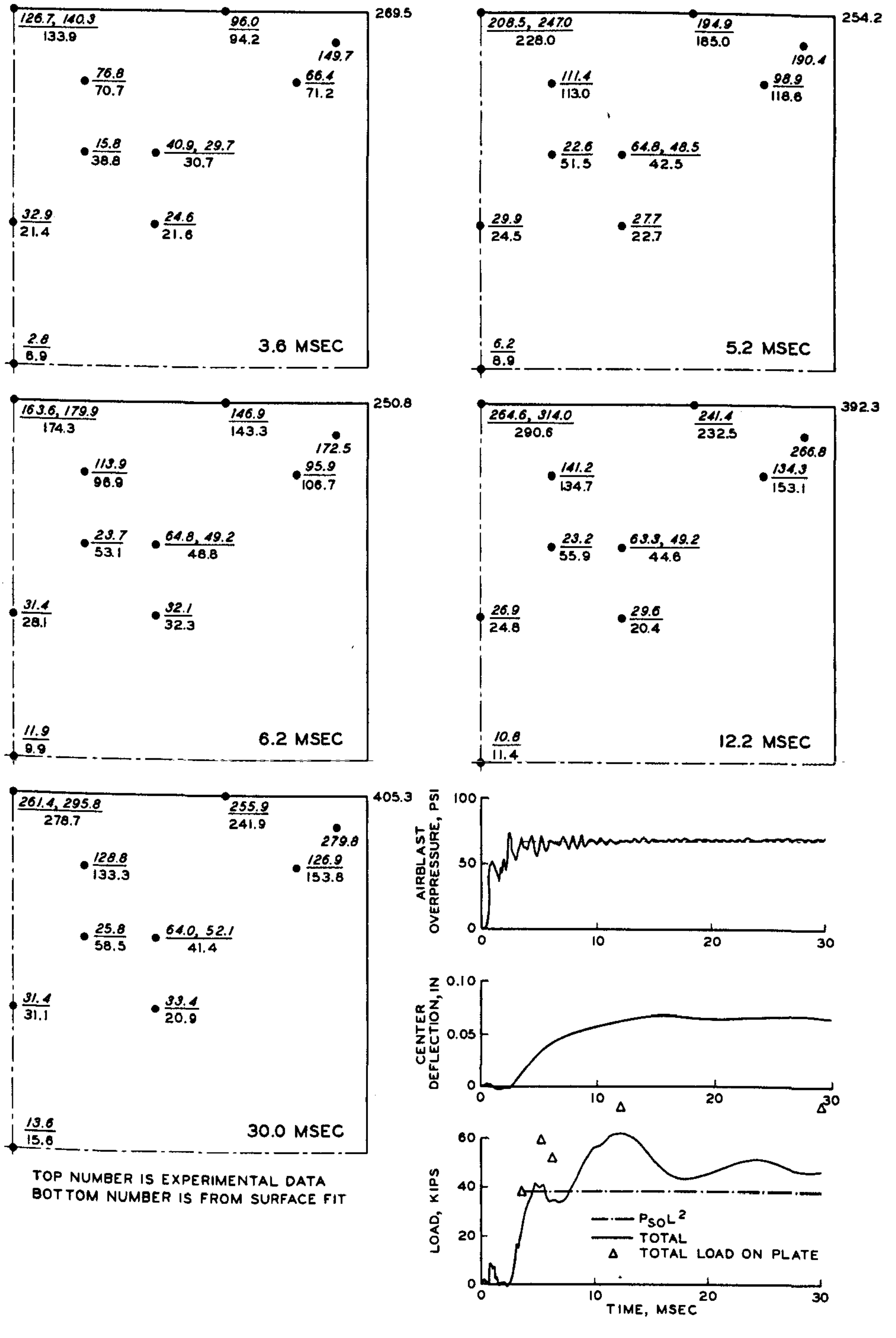

Fig. 31. Experimental data and surface fit values for dynamic test 3 at 12-in. depth of burial

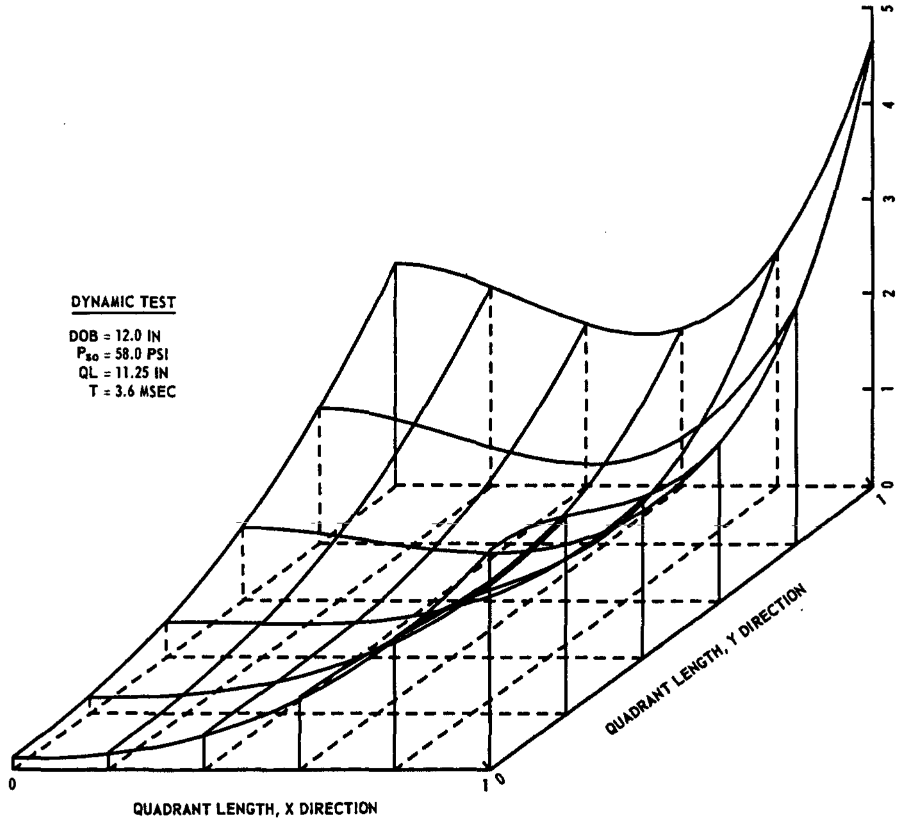

Fig. 32. Soil-stress distribution across one quadrant of plate for dynamic test 3 at 3.6 msec

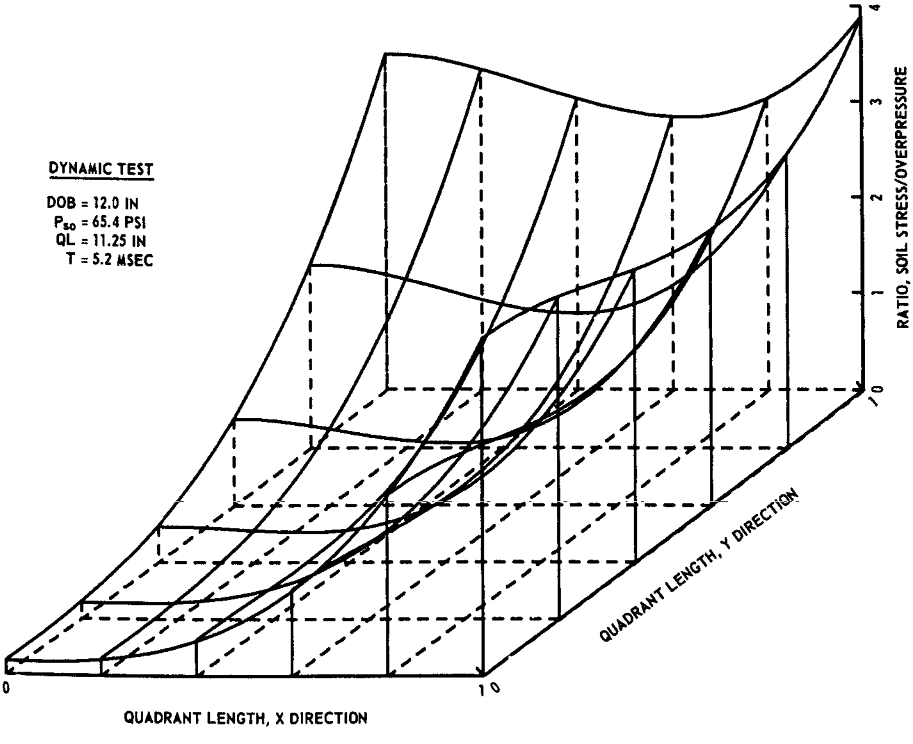

Fig. 33. Soil-stress distribution across one quadrant of plate for dynamic test 3 at 5.2 msec

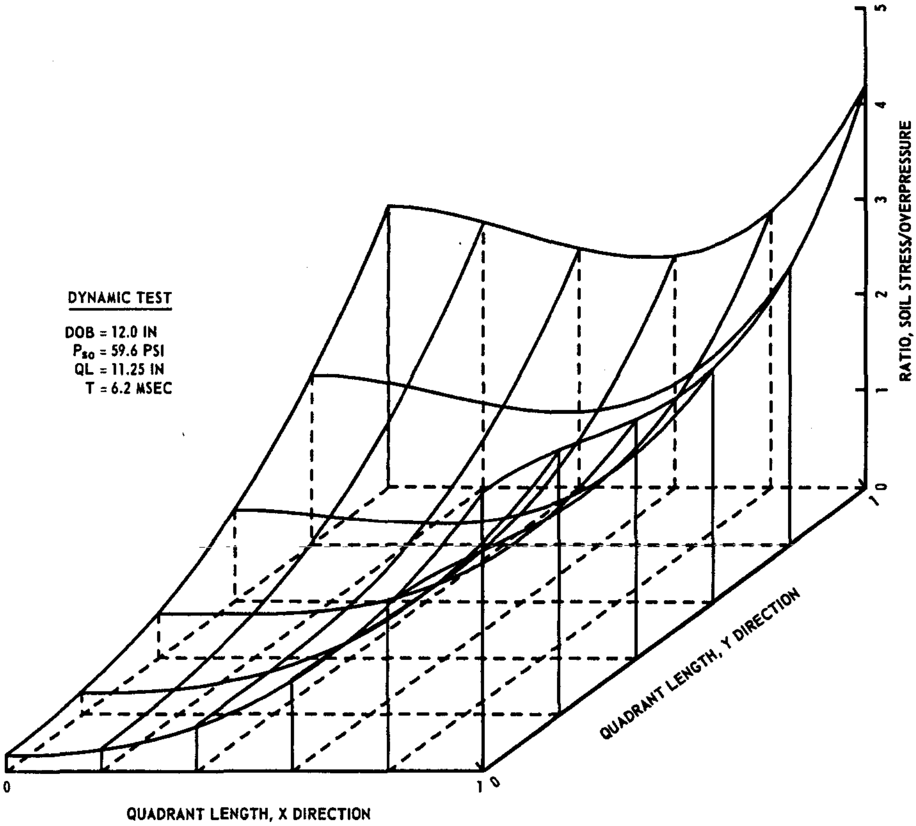

Fig. 34. Soil-stress distribution across one quadrant of plate for dynamic test 3 at 6.2 msec

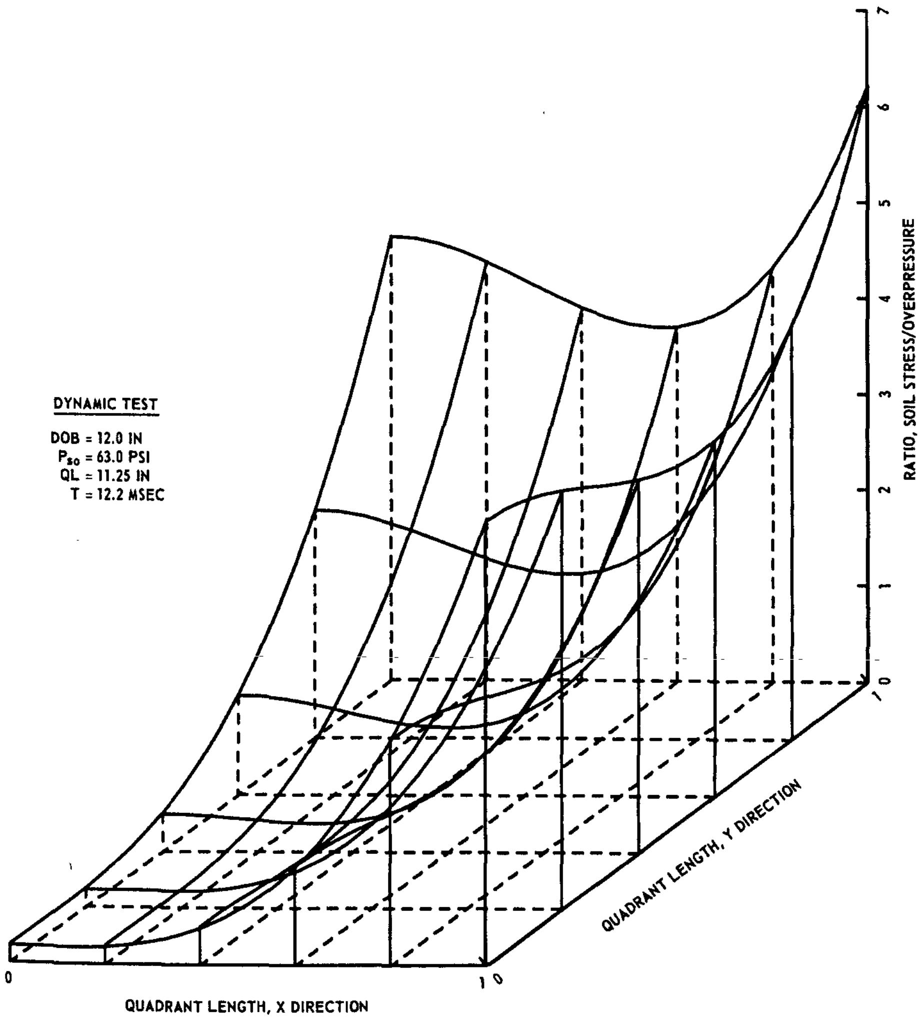

Fig. 35. Soil-stress distribution across one quadrant of plate for dynamic test 3 at 12.2 msec

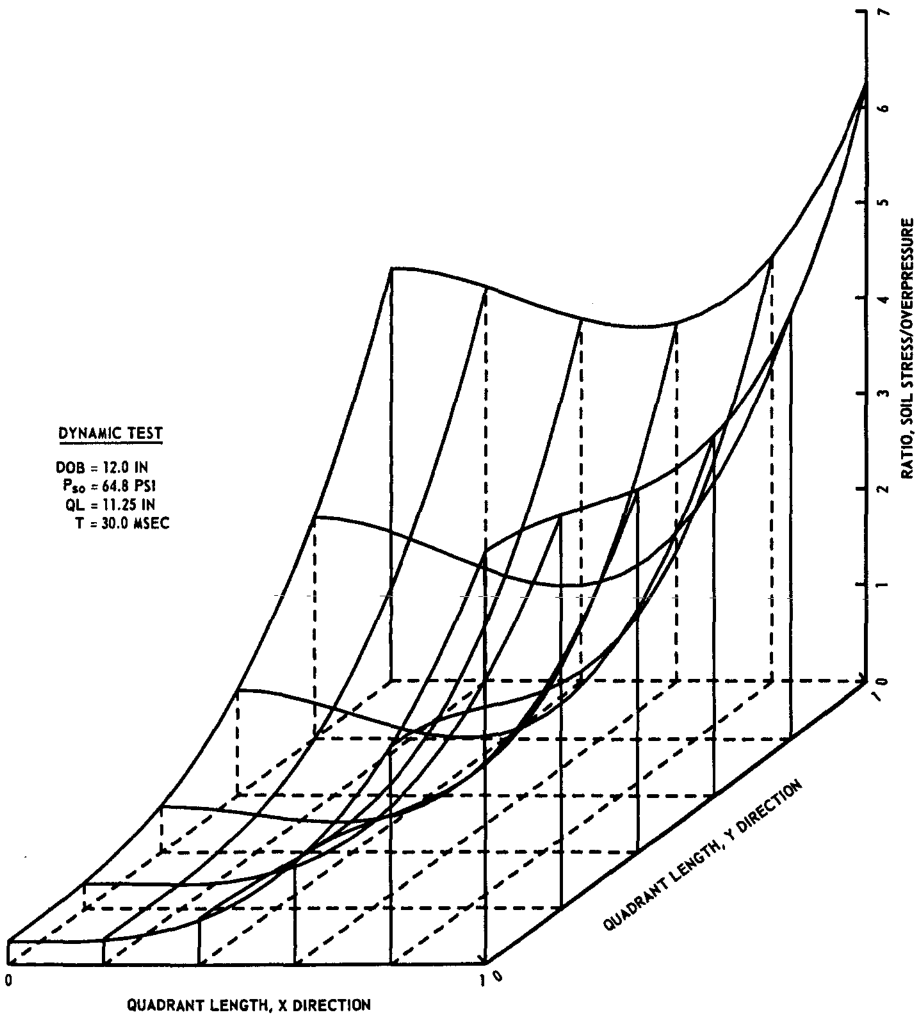

Fig. 36. Soil-stress distribution across one quadrant of plate for dynamic test 3 at 30.0 msec

greater than that when maximum deflection occurred in the plate (times greater than 15 msec for these tests).

4. The test assembly used in these tests together with the procedure for obtaining the total loads can be used for static in-place calibration of on-structure soil-stress gages.

5. The surface fit suitably represents the soil-stress distribution on the plate.

APPENDIX I.--REFERENCES

1. Albritton, G. E., "Description, Proof Test, and Evaluation of Blast Load Generator Facility," Technical Report No. 1-707, U. S. Army Engineer Waterways Experiment Station, CE, Vicksburg, Miss., Dec., 1965.

2. Dorris, A. F., "Response of Horizontally Oriented Buried Cylinders to Static and Dynamic Loading," thesis presented to the University of Illinois, at Urbana, Ill. in 1965, in partial fulfillment of the requirements for the degree of Doctor of Philosophy and published by U. S. Army Engineer Waterways Experiment Station, CE, Vicksburg, Miss., Technical Report No. 1-682, July, 1965.

3. Durbin, W. L., "Study of the Dynamic Stress-Strain and Wave-Propagation Characteristics of Soils; Measurements of Stress-Strain, Peak Particle Velocity, and Wave-Propagation Velocity in Three Sands," Contract Report No. 3-91, Report 3, U. S. Army Engineer Waterways Experiment Station, CE, Vicksburg, Miss., Feb., 1965; prepared by United Research Services Corporation, Burlingame, Calif., under Contract No. DA-22-079-eng-373.

4. Faust, R. W., and Ingram, J. K., "Development of On-Structure Stress Gages," Technical Report No. 1-801, U. S. Army Engineer Waterways Experiment Station, CE, Vicksburg, Miss., Nov., 1967.

5. Flathau, W. J., "Research in Soil Structure Interaction," Journal of the Structural Division, American Society of Civil Engineers, Vol. 91, No. ST4, Paper 4427, Aug., 1965, pp. 35-45.

6. Kennedy, T. E., Albritton, G. E., and Walker, R. E., "Initial Evaluation of the Free-Field Response of the Large Blast Load Generator," Technical Report No. 1-723, U. S. Army Engineer Waterways Experiment Station, CE, Vicksburg, Miss., June, 1966.

7. Mason, H. G., et al., "A Study of the Dynamic Soil-Structure Interaction Characteristics of Real Soil Media," Technical Documentary Report No. RTD TDR-63-3075, Air Force Weapons Laboratory, Kirtland AFB, N. Mex., Dec., 1966.

8. McNulty, J. W., "An Experimental Study of Arching in Sand," thesis presented to the University of Illinois, at Urbana, Ill. in 1965, in partial fulfillment of the requirements for the degree of Doctor of Philosophy and published by U. S. Army Engineer Waterways Experiment Station, CE, Vicksburg, Miss., Technical Report No. 1-674, May, 1965.

9. Meyer, G. D., and Flathau, W. J., "Static and Dynamic Tests of Unreinforced Concrete Fixed-End Arches Buried in Dry Sand," Technical Report No. 1-758, U. S. Army Engineer Waterways Experiment Station, CE, Vicksburg, Miss., Feb., 1967.

10. Natrella, M. G., "Experimental Statistics," Handbook 91, U. S. Department of Commerce, National Bureau of Standards, Aug., 1963.

11. Reiff, C. M., and Linger, D. A., "Investigation of Buried Domes, Phase I, Evaluation of Instrumentation and Preliminary Tests," Technical Report No. AFWL-TR-67-110, Air Force Weapons Laboratory, Kirtland AFB, N. Mex., Dec., 1967.

DISTRIBUTION LIST FOR NUCLEAR WEAPONS EFFECTS DIVISION REPORTS

Address	No. of Copies
Army	
Chief of Research and Development, Headquarters, Department of the Army ATTN: Director of Army Technical Information Washington, D. C. 20310	3 copies of Form 1473
Chief of Research and Development, Department of the Army	
ATTN: Atomic Office	1
CRDES	1
Washington, D. C. 20310	
Chief of Engineers, Department of the Army	
ATTN: ENGTE-S	1
ENGTE-M	1
ENGTE-E	1
ENGCW-E	1
ENGCW-Z	1
ENGMC-E	1
ENGMC-EM	1
ENGMC-DE	1
ENGMC-M	1
ENGAS-I	2
ENGNA	1
Washington, D. C. 20315	
Department of the Army CE Ballistic Missile Construction Office P. O. Box 4187 Norton AFB, Calif. 92409	1
Director U. S. Army Terrestrial Sciences Research ATTN: Mr. K. Boyd P. O. Box 282 Hanover, N. H. 03755	1
Division Engineers, U. S. Army Engineer Divisions Continental United States	Cy to ea

Address	No. of Copies
Army (Continued)	
Director, Technical Documents Center Evans Signal Laboratory Belmar, N. J. 07719	1
Commanding General, U. S. Army Materiel Command ATTN: AMCRD-DE-N Washington, D. C. 20310	2
Director of Civil Defense, Office of the Secretary of the Army, ATTN: Mr. George Sisson (RE-ED) Washington, D. C. 20310	2
Commanding General, U. S. Continental Army Command Fort Monroe, Va. 23351	1
President, U. S. Army Air Defense Board Fort Bliss, Tex. 79906	1
Commandant, U. S. Army Air Defense School Fort Bliss, Tex. 79906	1
Commandant, U. S. Army Command & General Staff College ATTN: Archives Ft. Leavenworth, Kans. 66027	1
Commanding Officer, U. S. Army Combat Developments Command, Institute of Nuclear Studies Fort Bliss, Tex. 79916	2
Commanding General, Aberdeen Proving Ground ATTN: Director, Ballistic Research Laboratories Aberdeen, Md. 21005	4
Commanding General, The Engineer Center ATTN: Assistant Commandant, Engineer School Fort Belvoir, Va. 22060	1

Address	No. of Copies
Army (Continued)	
Commanding Officer, U. S. Army Mobility Equipment Research and Development Center ATTN: Technical Documents Center, Building 315 Ft. Belvoir, Va. 22060	1
Director, U. S. Army Mobility Equipment Research and Development Center ATTN: Chief, Technical Support Branch Ft. Belvoir, Va. 22060	1
Commanding Officer, Picatinny Arsenal ATTN: ORDBB-TK Dover, N. J. 07801	1
Commanding Officer, Transportation Research Command ATTN: Chief, Technical Information Division Fort Eustis, Va. 23604	1
Commanding General, U. S. A. Electronic R&D Laboratory ATTN: Technical Documents Center, Evans Area Ft. Monmouth, N. J. 07703	1
Commanding General, USA Missile Command Huntsville, Ala. 35809	1
Commanding General, USA Munition Command Dover, N. J. 07801	1
Director, U. S. Army Corps of Engineers, Coastal Engineering Research Center ATTN: Mr. T. Saville, Jr. Washington, D. C. 20315	1
Commanding Officer, U. S. Army Nuclear Defense Laboratory ATTN: Technical Library Edgewood Arsenal, Edgewood, Md. 21040	1

Address	No. of Copies
Army (Continued)	
Director, U. S. Army Corps of Engineers, Ohio River Division Laboratories, 5851 Mariemont Avenue Cincinnati, Ohio 45227	1
District Engineer, U. S. Army Engineer District, Omaha 6012 U. S. Post Office and Court House, 215 N. 17th Street ATTN: MROGS-B Omaha, Nebr. 68101	1
U. S. Army Engineer Division, Missouri River P. O. Box 103, Downtown Station ATTN: Mr. Ken Lane Omaha, Nebr. 68101	1
Commandant, Army War College ATTN: Library Carlisle Barracks, Pa. 17013	1
Superintendent, U. S. Military Academy ATTN: Library West Point, N. Y. 10996	2
Director, Nuclear Cratering Group, U. S. Army Corps of Engineers, Lawrence Radiation Laboratory P. O. Box 808, Livermore, Calif. 94550	1
Navy	
Chief of Naval Operations, Navy Department	
ATTN: OP-75	2
OP-03EG	1
Washington, D. C. 20350	

Address	No. of Copies
Navy (Continued)	
Director of Naval Intelligence, Navy Department ATTN: OP-922V Washington, D. C. 20350	1
Special Projects, Navy Department ATTN: SP-272 Washington, D. C. 20360	1
Commander, Naval Ordnance Systems Command Washington, D. C. 20360	1
Commander, Naval Ship Engineering Center ATTN: Code 6115 Washington, D. C. 20360	1
Commander, Naval Facilities Engineering Command, Navy Dept	
ATTN: Code 04	1
Code 03	1
Washington, D. C. 20370	
Chief of Naval Research, Navy Department ATTN: Code 811 Washington, D. C. 20390	1
Commander-in-Chief, Pacific, FPO San Francisco, Calif. 94129	1
Commander-in-Chief, U. S. Atlantic Fleet, U. S. Naval Base Norfolk, Va. 23511	1
Commandant of the Marine Corps, Navy Department ATTN: Code A03H Washington, D. C. 20380	4

Address	No. of Copies
Navy (Continued)	
President, U. S. Naval War College Newport, R. I. 02840	1
Commanding Officer, Nuclear Weapons Training Center ATTN: Nuclear Warfare Department Atlantic Naval Base, Norfolk, Va. 23511	1
Commanding Officer, U. S. Naval Schools Command U. S. Naval Station, Treasure Island San Francisco, Calif. 94130	1
Commanding Officer, U. S. Naval Weapons Laboratory ATTN: TE Dahlgren, Va. 22448	1
Commanding Officer, U. S. Naval Weapons Evaluation Facility ATTN: Code WEVS, Kirtland Air Force Base Albuquerque, N. Mex. 87117	1
Commander, U. S. Naval Oceanographic Office Suitland, Md. 20390	1
Officer-in-Charge, U. S. Naval Civil Engineer Corps Officer School, U. S. Naval Construction Battalion Center Port Hueneme, Calif. 93041	1
Superintendent, U. S. Naval Postgraduate School Monterey, Calif. 93940	1
Commanding Officer, Nuclear Weapons Training Center, Pacific, Naval Station, North Island San Diego, Calif. 92136	2
Commanding Officer, U. S. Naval Damage Control Training Center, Naval Base, ATTN: ABC Defense Course Philadelphia, Pa. 19112	1

Address	No. of Copies
Navy (Continued)	
Commander, U. S. Naval Ordnance Laboratory	
ATTN: EA	1
EU	1
E	1
Silver Spring, Md. 20910	
Commander, U. S. Naval Ordnance Test Station China Lake, Calif. 93555	1
Commanding Officer & Director, U. S. Naval Civil Engineering Laboratory, ATTN: Code L31 Port Hueneme, Calif. 93041	2
Director, U. S. Naval Research Laboratory Washington, D. C. 20390	1
Commanding Officer & Director, Naval Electronics Laboratory San Diego, Calif. 92152	1
Commanding Officer, U. S. Naval Radiological Defense Laboratory, ATTN: Technical Information Division San Francisco, Calif. 94129	1
Commanding Officer & Director Naval Ship Research and Development Center Carderock, Md. 20007	1
Underwater Explosions Research Division Naval Ship Research and Development Center Norfolk Naval Shipyard Portsmouth, Va. 23511	1
Air Force	
Director, Air Research and Development Command, Headquarters, USAF, ATTN: Combat Components Division Washington, D. C. 20330	1

Address	No. of Copies
Air Force (Continued)	
Headquarters, USAF ATTN: AFRSTG, Washington, D. C. 20330	1
Commander, Tactical Air Command ATTN: Document Security Branch Langley AFB, Va. 23365	1
Commander, Air Force Logistics Command Wright-Patterson AFB, Ohio 45433	2
Air Force Systems Command, Andrews Air Force Base ATTN: RDRWA, Washington, D. C. 20331	1
Director, Air University Library Maxwell AFB, Ala. 36112	2
AFCRL, L. G. Hanscom Field ATTN: CRQST-2 Bedford, Mass. 01731	1
AFWL ATTN: Library WLDC Kirtland AFB, N. Mex. 87117	 2 1
Air Force Institute of Technology AFIT-L, Bldg 640 Wright-Patterson AFB, Ohio 45433	1
Space and Missile Systems Organization ATTN: SAMSO (SMQNM) Norton AFB, Calif. 92409	1

NWED Reports Distribution List

Address	No. of Copies
Air Force (Continued)	
Commander, Strategic Air Command ATTN: OAWS, Offutt AFB, Nebr. 68113	1
Director, U. S. Air Force Project RAND, Via: U. S. Air Force Liaison Office, The RAND Corporation, 1700 Main Street	
ATTN: Library	1
Dr. Harold L. Brode	1
Dr. Olen A. Nance	1
Santa Monica, Calif. 90406	
Director of Civil Engineering, Headquarters, USAF ATTN: AFOCE Washington, D. C. 20330	1
Air Force Flight Dynamics Laboratory Wright-Patterson AFB ATTN: Mr. Frank Janik, Jr. Dayton, Ohio 45433	1
Air Force Technical Applications Center Department of the Air Force Washington, D. C. 20333	1
Other DOD Agencies	
Defense Documentation Center (DDC), ATTN: Mr. Myer Kahn Cameron Station, Alexandria, Va. 22314 (NO TOP SECRET TO THIS ADDRESS)	20
Director, Defense Atomic Support Agency ATTN: SPSS, Washington, D. C. 20301	5
Director of Defense Research and Engineering	
ATTN: Technical Library	1
Mr. Frank J. Thomas	1
Washington, D. C. 20301	

Address	No. of Copies
Other DOD Agencies (Continued)	
Assistant to the Secretary of Defense (Atomic Energy) Washington, D. C. 20301	1
U. S. Documents Officer, Office of the United States National Military Representative-SHAPE APO New York 09055	1
Director, Weapons Systems Evaluation Group Washington, D. C. 20305	1
Commandant, Armed Forces Staff College ATTN: Library Norfolk, Va. 23511	1
Commander, Field Command, DASA Sandia Base, Albuquerque, N. Mex. 87115	2
Commander, Test Command, DASA, ATTN: TCCOM, TCDT Sandia Base, Albuquerque, N. Mex. 87115	2
Commandant, The Industrial College of the Armed Forces Ft. McNair, Washington, D. C. 20310	1
Commandant, National War College ATTN: Class Rec. Library Washington, D. C. 20310	1
Director, Advanced Research Projects Agency ATTN: NTDO, Washington, D. C. 20301	1
Director, Defense Intelligence Agency ATTN: DIAAP-IK2, Washington, D. C. 20301	1
U. S. Atomic Energy Commission ATTN: Chief, Classified Tech Lib, Tech Information Service Washington, D. C. 20545	1

Address	No. of Copies
Other DOD Agencies (Continued)	
Manager, Albuquerque Operations Office, USAEC P. O. Box 5400 Albuquerque, N. Mex. 87115	1
Manager, Nevada Operations Office, USAEC, P. O. Box 1676 Las Vegas, Nev. 89101	1
National Military Command System Support Center Pentagon BE 685, ATTN: Technical Library Washington, D. C. 20301	1
Dr. John S. Rinehart Senior Research Fellow (R.2), IER/ESSA Boulder, Colo. 80302	1
Administrator, National Aeronautics & Space Administration 400 Maryland Avenue, S. W. Washington, D. C. 20546	1
National Aeronautics & Space Administration, Man-Spacecraft Center, Space Technology Division, Box 1537 Houston, Tex. 77001	1
Langley Research Center, NASA, Langley Field ATTN: Mr. Philip Donely Hampton, Va. 23365	1
Other Agencies	
University of California, Lawrence Radiation Laboratory P. O. Box 808, ATTN: Technical Information Division Livermore, Calif. 94550	2
Los Alamos Scientific Laboratory, P. O. Box 1663 ATTN: Report Librarian Los Alamos, N. Mex. 87544	1

Address	No. of Copies
Other Agencies (Continued)	
Massachusetts Institute of Technology, Division of Sponsored Research, 77 Massachusetts Avenue	
ATTN: Dr. Robert J. Hansen	1
Dr. Robert V. Whitman	1
Cambridge, Mass. 02139	
Sandia Corporation, P. O. Box 5800	1
ATTN: Classified Document Division for Dr. M. L. Merritt	
Albuquerque, N. Mex. 87115	
University of Illinois, Urbana Campus	
ATTN: Professor N. M. Newmark	1
Professor J. L. Merritt	1
Professor M. T. Davisson	1
Professor G. K. Sinnamon	1
Professor W. J. Hall	1
Professor A. J. Hendron, Jr.	1
Professor M. Sozen	1
Department of Civil Engineering	
Urbana, Ill. 61801	
General Electric Company, Missile and Space Vehicle Department, Valley Forge Space Technology Center	1
Goddard Boulevard	
King of Prussia, Pa. 19406	
U. S. Department of the Interior, Geological Survey	1
Geologic Division, Branch of Engineering Geology	
ATTN: Harold W. Olsen, 345 Middlefield Road	
Menlo Park, Calif. 94025	
URS Corporation, 1811 Trousdale Drive	2
ATTN: Mr. Harold Mason	
Burlingame, Calif. 94010	

Address	No. of Copies
Other Agencies (Continued)	
Stanford Research Institute	1
ATTN: Mr. Fred M. Sauer	
Menlo Park, Calif. 94025	
General American Transportation Corporation	1
General American Research Division	
7449 North Natchez Avenue, ATTN: Dr. G. L. Neidhardt	
Niles, Ill. 60648	
IIT Research Institute, 10 West 35th Street	1
ATTN: Dr. T. Schiffman	
Chicago, Ill. 60616	
Paul Weidlinger, Consulting Engineer, 777 Third Avenue	1
ATTN: Dr. M. L. Baron	
New York, N. Y. 10017	
~~Engineering Physics Company, 12721 Twinbrook Parkway~~	
ATTN: Dr. Vincent J. Cushing	1
Mr. W. Danek	1
Rockville, Md. 20852	
Lockheed Missile and Space Company	1
Lockheed Aircraft Corporation, 111 Lockheed Way	
ATTN: Dr. R. E. Meyerott	
Sunnyvale, Calif. 94086	
TRW Space Technology Laboratories, One Space Park	
ATTN: Dr. Millard Barton	1
Mr. M. V. Anthony	1
Redondo Beach, Calif. 90278	
Edgerton, Germeshausen & Grier, Inc.	1
95 Brookline Avenue, ATTN: D. F. Hansen	
Boston, Mass. 02129	

Address	No. of Copies
Other Agencies (Continued)	
General Electric Company, TEMPO, 816 State Street ATTN: Mr. Warren Chan (DASIAC) Santa Barbara, Calif. 93101	1
Battelle Memorial Institute 505 King Avenue ATTN: Mr. R. W. Klingesmith Columbus, Ohio 43201	1
Technical Operations, Inc., South Avenue ATTN: Dr. Paul I. Richards Burlington, Mass. 01803	1
AVCO Corporation, Research and Advanced Development Division, 201 Lowell Street ATTN: Mr. R. E. Cooper Wilmington, Mass. 01887	1
The Mitre Corporation, Route 62 and Middlesex Turnpike Bedford, Mass. 01730	1
Agbabian-Jacobsen Associates, Engineer Consultants 8939 South Sepulveda Boulevard, Suite 340 Los Angeles, Calif. 90045	1
Defense Research Corporation, P. O. Box 3587 ATTN: Mr. Benjamin Alexander Santa Barbara, Calif. 93105	1
General Atomic, Division of General Dynamic Corporation P. O. Box 111, 10955 John Jay Hopkins Drive ATTN: Dr. K. D. Pyatt, Jr. San Diego, Calif. 92112	1
Applied Theory, Inc., 1950 Cotner Avenue ATTN: Dr. John C. Trulio West Los Angeles, Calif. 90025	1

Address	No. of Copies
Other Agencies (Continued)	
Physics International Company, 2700 Merced Street ATTN: Dr. Charles Godfrey San Leandro, Calif. 94577	1
Aerospace Corporation, 1111 E. Mill Street ATTN: Dr. M. B. Watson San Bernardino, Calif. 92408	1
Dynamic Science Corporation, 1900 Walker Avenue ATTN: Dr. J. C. Peck Monrovia, Calif. 91016	1
Ministry of Defense, MEXE, Christchurch	
ATTN: Dr. Philip S. Bulson	1
Mr. Bruce T. Boswell Hampshire, England	1
Defence Research Establishment, Suffield Ralston, Alberta, Canada	1
Corrugated Metal Pipe Institute ATTN: Mr. W. A. Porter Crestview Plaza, Port Credit Ontario, Canada	1
Denver Mining Research Center Building 20, Denver Federal Center ATTN: Dr. Leonard A. Obert Denver, Colo. 80225	1
Research Analysis Corporation Document Control Supervisor McLean, Va. 22101	1
University of Detroit, Department of Civil Engineering 4001 West McNichols Road ATTN: Professor W. J. Baker Detroit, Mich. 48221	1

Address	No. of Copies
Other Agencies (Continued)	
Kondner Research, Downes Road ATTN: Dr. R. L. Kondner Parkton, Md. 21120	1
Dr. Eugene Zwoyer Eric H. Wang Civil Engr Research Facility University of New Mexico Albuquerque, N. Mex. 87106	1
University of Arizona ATTN: Dr. George Howard Tucson, Ariz. 85721	1
Florida State University, Department of Engineering Science ATTN: Dr. G. L. Rogers Tallahassee, Fla. 32306	1
Lehigh University	
ATTN: Dr. J. F. Libsch, Materials Research Center	1
Dr. D. A. Van Horn, Department of Civil Engineering Bethlehem, Pa. 18015	1
Nova Scotia Technical College, School of Graduate Studies ATTN: Dr. G. G. Meyerhof Halifax, Nova Scotia, Canada	1
Worcester Polytechnic Institute, Department of Civil Engrg ATTN: Dr. Carl Koontz Worcester, Mass. 01609	1
Pennsylvania State University, 101 Eng. A ATTN: Professor Richard Kummer University Park, Pa. 16802	1
Penn State University ATTN: Professor G. Albright University Park, Pa. 16802	1

Address	No. of Copies
Other Agencies (Continued)	
University of Florida, Department of Mechnical Engineering ATTN: Professor John A. Samuel Gainesville, Fla. 32603	1
Purdue University, School of Civil Engineering Civil Engineering Building ATTN: Professor M. B. Scott Lafayette, Ind. 47907	1
Nuclear Defense Design Center School of Engineering and Applied Science The George Washington University Washington, D. C. 20006	1
University of Colorado, School of Architecture ATTN: Professor G. K. Vetter Boulder, Colo. 80304	1
San Jose State College, Department of Civil Engineering ATTN: Dr. Franklin J. Agardy San Jose, Calif. 95114	1
University of Washington, Department of Civil Engineering 307 More Hall ATTN: Professor William Miller Seattle, Wash. 98105	1
Bell Telephone Laboratories, Inc., Whippany Road ATTN: Mr. R. W. Mayo Whippany, N. J. 07981	1
Utah State University, Department of Mechanical Engineering ATTN: Professor R. K. Watkins Logan, Utah 84321	1
Iowa State University of Science and Technology ATTN: Professor Glen Murphy Ames, Iowa 50010	2

Address	No. of Copies
Other Agencies (Continued)	
University of Michigan, Civil Engineering Department ATTN: Professor Frank E. Richart, Jr., Consultant Ann Arbor, Mich. 48104	1
Southwest Research Institute, 8500 Culebra Road ATTN: Dr. Robert C. DeHart San Antonio, Tex. 78228	1
University of Washington, Department of Civil Engineering ATTN: C. H. Norris, Department of Civil Engineering Seattle, Wash. 98105	1
Rice University, Department of Civil Engineering ATTN: Professor A. S. Veletsos Houston, Tex. 77001	1
University of Washington, Department of Physics ATTN: Dr. A. B. Arons Seattle, Wash. 98105	1
Balcones Research Center, University of Texas ATTN: Dr. J. Neils Thompson Austin, Tex. 78712	1
University of Massachusetts, Department of Civil Engineering, ATTN: Dr. M. P. White Amherst, Mass. 01002	1
Rensselaer Polytechnic Institute ATTN: Dr. Clayton Oliver Dohrenwend, Security Officer Mason House, Troy, N. Y. 12180	1
University of New Mexico Civil Engineering Research Facility P. O. Box 188, University Station Albuquerque, N. Mex. 87106	2

Address	No. of Copies
Other Agencies (Continued)	
The Boeing Company, P. O. Box 3707 ATTN: Technical Library Seattle, Wash. 98124	1
Dr. George B. Clark, Director, Rock Mechanics Research Group, University of Missouri at Rolla Rolla, Mo. 65401	1
Dr. Donald A. Da Deppo, Engineering Mechanics Department, University of Detroit McNichols Road at Livernois Detroit, Mich. 48221	1
Prof. Bruce G. Johnston Department of Civil Engineering University of Arizona Tucson, Ariz. 85721	1

Unclassified

Security Classification

DOCUMENT CONTROL DATA - R & D

(Security classification of title, body of abstract and indexing annotation must be entered when the overall report is classified)

1. ORIGINATING ACTIVITY (Corporate author) U. S. Army Engineer Waterways Experiment Station Vicksburg, Mississippi	2a. REPORT SECURITY CLASSIFICATION Unclassified 2b. GROUP

3. REPORT TITLE

PRESSURE DISTRIBUTION ON A BURIED FLAT PLATE SUBJECTED TO STATIC AND AIRBLAST OVERPRESSURES

4. DESCRIPTIVE NOTES (Type of report and inclusive dates)

Final report

5. AUTHOR(S) (First name, middle initial, last name)

Jimmy P. Balsara
Reid S. Cummins, Jr.

6. REPORT DATE	7a. TOTAL NO. OF PAGES	7b. NO. OF REFS
October 1968	47	11

8a. CONTRACT OR GRANT NO.	9a. ORIGINATOR'S REPORT NUMBER(S) Miscellaneous Paper N-68-4
b. PROJECT NO.	
c.	9b. OTHER REPORT NO(S) (Any other numbers that may be assigned this report)
d.	

10. DISTRIBUTION STATEMENT

This document has been approved for public release and sale; its distribution is unlimited.

11. SUPPLEMENTARY NOTES	12. SPONSORING MILITARY ACTIVITY
	Defense Atomic Support Agency Washington, D. C.

13. ABSTRACT

The objectives of this study were to develop and represent the pressure distribution on the surface of a buried, simply supported flat plate subjected to static and airblast overpressures. The plate was 24 in. square and buried in dense, dry sand to a depth of one-half span, and subjected to static surface overpressures ranging from 0 to 75 psi and airblast overpressures at the surface ranging from 29 to 65 psi. The plate was instrumented with thirteen soil-stress gages to measure the soil-stress or pressure distribution, and a load cell was used to measure the total reaction of the plate. A surface represented by a third order polynomial was fitted to the experimental data to represent graphically the pressure distribution and to facilitate the computation of the value (force) of the volume under the surface so that it could be compared with the value of force measured by the reaction load cell. The results indicate that the load on the plate, for both the static test and the dynamic test for times when the comparison was valid, was considerably greater than the reaction. The static soil stress, represented in nondimensional form as the ratio of soil stress to overpressure, remains relatively constant during loading but increases during unloading. The dynamic soil-stress overpressure ratio, above a certain overpressure level, increases from below unity at the center of the plate to above unity at the supports, and the distribution and variation with time essentially remain the same.

DD FORM 1 NOV 65 1473 REPLACES DD FORM 1473, 1 JAN 64, WHICH IS OBSOLETE FOR ARMY USE.

Unclassified

Security Classification

14. KEY WORDS	LINK A		LINK B		LINK C	
	ROLE	WT	ROLE	WT	ROLE	WT
Air blast						
Buried plates						
Overpressures						
Pressure Distribution						
Soil stresses						